agronomy

Article

Microanatomical Properties of Energy Willow (*Salix* spp.) Leaves after Exposure to Potentially Toxic Elements from Wastewater Solids and Wood Ash

Csilla Tóth [1], László Simon [1] and Brigitta Tóth [2,*]

[1] Department of Agricultural Sciences and Environmental Management, Institute of Engineering and Agricultural Sciences, University of Nyíregyháza, Sostoi Str. 31/b, H-4400 Nyiregyhaza, Hungary; toth.csilla@nye.hu (C.T.); simon.laszlo@nye.hu (L.S.)
[2] Institute of Food Science, Faculty of Agricultural and Food Sciences and Environmental Management, University of Debrecen, Boszormenyi Str. 138, H-4032 Debrecen, Hungary
* Correspondence: btoth@agr.unideb.hu; Tel.: + 36-30-2738842

Abstract: This open-field small-plot long-term experiment was set up between 2011 and 2021 with willow (*Salix triandra* × *S. viminalis* 'Inger'), grown as a short rotation coppice energy crop in Nyíregyháza, Hungary. The sandy loam Cambisol was treated with wastewater solids (WS) in the form of municipal sewage sludge compost (MSSC, 2011, 2013, and 2016), municipal sewage sediment (MSS, 2018), and with willow ash (WA, 2011, 2013, 2016, and 2018). Control plots remained untreated since 2011. All soil treatments significantly enhanced the uptake or accumulation of potentially toxic elements (PTEs) in the leaves of willows. During June 2019, 53 weeks after the last soil treatments, MSSC + MSS-, WA-, and MSSC + MSS + WA-treated willows leaves had 14–68% more As, 17–48% more Ba, 31–104% more Cr, 4–12% more Cu, 6–15% more Mn, 18–218% more Pb, and 11–35% more Zn compared to the untreated control. Significantly higher Mn and Zn concentrations were measured in the MSSC + MSS + WA treatments than in the MSSC + MSS treatments. The assumption that WA reduces the accumulation of PTEs in willow leaves when applied together with MSSC and MSS was therefore only partially confirmed. The hypothesis of this study was that PTEs accumulated in the leaves would affect the microanatomical parameters of the leaves. Numerous positive changes were observed with the combined application of WS and WA. MSSC + MSS + WA treatment reduced the thickness of the mesophyll less than MSSC + MSS or WA treatments alone; the size of the cells building the palisade and spongy parenchyma and the extent of the main vein significantly increased. In the case of the combined treatment, the extent of the sclerenchymatous stock was smaller than in the control but larger than in WS- or WA-treated willow. The extent of the collenchymatous stock significantly increased compared to the control. Increases in the thickness of the adaxial epidermis and the number of stomata were statistically significant. However, the extent of the increases did not reach the extent of the increase experienced in the case of WS treatment, as the size of the stomata did not significantly decrease.

Keywords: energy willow (*Salix* spp.); leaf microanatomy; potentially toxic elements; wastewater solids; wood ash

check for updates

Citation: Tóth, C.; Simon, L.; Tóth, B. Microanatomical Properties of Energy Willow (*Salix* spp.) Leaves after Exposure to Potentially Toxic Elements from Wastewater Solids and Wood Ash. *Agronomy* **2024**, *14*, 1625. https://doi.org/10.3390/agronomy14081625

Academic Editor: Changfeng Ding

Received: 29 June 2024
Revised: 23 July 2024
Accepted: 23 July 2024
Published: 25 July 2024

1. Introduction

Among perennial energy crops, which are cultivated for high aboveground biomass, the high-yielding, rapidly growing willow (*Salix*) species are promising all over the world. Since short-rotation coppice (SRC) energy plantations can be cultivated for 15–20 years in the same field, a balanced and regular nutrient supply is required for good aboveground biomass yields [1,2].

The biomass yield of *Salix* spp., grown as an energy crop, can be stimulated by the application of various inorganic or organic fertilizers and additives in the soil, including biosolids (e.g., municipal sewage sludge) or biomass ash [3–7]. Application of various soil amendments (e.g., municipal sewage sludge or wood ash) can enhance not only the uptake rate of beneficial elements (e.g., nitrogen or potassium) but also the rate of accumulation of potentially toxic elements (PTEs) in the willow's organs [4,5,8–13]. Besides leaves, PTEs can also accumulate in the harvested shoots of willows. Since shoots are burned in biomass power plants, there is a danger that PTEs are enriched in the ash produced after burning.

It is well-documented that the Cd accumulation or Zn uptake rates of *Salix* spp. are high compared to other plant species and other trace elements [2,9,11,14–17]. Resistance or tolerance of willows to other metals (Cr, Cu, Ni, and Pb) and accumulation of elevated levels of As, Cu, Fe, Ni, Mn, and Pb [2,8,9,11,16–24] were also observed in the organs of various *Salix* spp. Therefore, from a phytoremediation point of view, the elevated levels of certain toxic elements could be advantageous in the shoots of SRC willow to remove metal pollutants from the soil [25,26].

Leaves have an important role in extracting PTEs from soil contaminants [27]. In the case of toxic element accumulation, leaf physiology can be impaired. Examining the effects of toxic elements on the microanatomy of leaves helps us to understand the tolerance mechanisms of vascular plants to heavy metal stress.

The toxic elements in the soil have strong histological effects on the plant, which can be seen in the alteration of the microanatomical parameters of the leaf, stem, and root. The toxic element content of the various organs correlates to the alterations of tissue structure [28–32]. These authors reported the following histological parameters in the case of leaves, which indicate the presence of toxic elements: thickness of the cuticle; stomata density and size; trichomes; the evolution of the typical characteristics of the epidermis; the evolution of the shape and cell wall of the cells of the collenchyma; the shape and size of the calcium oxalate crystals and the presence of druses in the cells of the collenchyma bordering the leaf veins; the ratio of palisade and spongy parenchyma in the mesophyll; and the thickness of the cell wall of the mesophyll cells. Hermle et al. [33] state that in the case of the leaves of *Salix viminalis* L. and *Populus tremula* L., the cells building the abaxial epidermis collapse as a result of heavy metal accumulation, the stomata shrink, the cells of the spongy parenchyma grow old, the chemical composition of the cell wall changes, and the lignin and pectin content of the cell walls increases, although their thickness decreases. As a result of their examination, they discovered the disruption of cell contents, the presence of phenolic compounds, condensation of cell remnants, thickening of cell walls, and partial cell epidermis collapse.

In the case of *Acer pseudopatanus*, André et al. [34] observed the degeneration of the palisade and spongy parenchyma. It was concluded that toxic elements, for example, zinc, were stored homogeneously in the cell wall of collenchyma. In particular, they accumulate in the pectin-rich outer layer of lower epidermis cells. Vollenweider et al. [35] also observed alterations in the leaf structure of *Salix viminalis*, which were induced by cadmium pollution. Growth of the vacuole of the cells of the palisade and the build-up of spongy parenchyma were observed in the leaf mesophyll. Nikolić et al. [36] examined two *Populus* clones. They stated that palisade cell size was considerably, but differentially, changed in both clones under Cd exposure: palisade cell size was decreased in *Populus* × *euramericana* but increased in *P. deltoides*. In their study, the decrease in palisade cell area and the reduction of mesophyll cell size were observed in the *Populus* × *euramericana* clone, similar to the observation of Di Baccio et al. [37]. Their results, as well as those of Luković et al. [38], showed that Cd treatment reduced adaxial epidermis cell size.

Similar to Shi and Cai [39], Nikolić et al. [36] also concluded that there is only limited information in the literature on the effect of heavy metal stress on the anatomic structure of leaves. In several woody plants, biomass production is known to be potentially sustained despite the structural changes to the microanatomy of leaf lamina. At the same time, they can remove pollutants from contaminated soils or render them harmless [40]. Thicknesses of the spongy and palisade parenchyma are associated with biomass production, and these parameters can be used as indicators of growth potential in these plants [41]. The interrelation between micromorphological parameters and PTE uptake capacity is useful for the identification of plants that are capable of phytoremediation [38].

Publications have pointed out that parallel to soil pollution, the thickness of the leaf lamina significantly decreases, the extent of the intercellular space changes, and so does the organization of the cells [42,43]. The publications mention other microanatomical parameters as indicators for measuring polluting effects: the thickness of the leaf plate, the height and width of the cells building up the upper epidermis, the size of the stomata, and the value of stomata density. Guo et al. [29] point out that the decrease in the size of the stomata is parallel to the increase in the value of stomatal density.

Considering the above preliminaries, the goal of this study was to investigate the uptake or accumulation of nine selected PTEs, As, Ba, Cd, Cr, Cu, Mn, Ni, Pb, and Zn, in the leaves of energy willow (*Salix triandra* × *S. viminalis* 'Inger') grown in a long-term experiment. It was assumed that repeated soil application of a combination of MSSC and MSS, along with WA, will influence the accumulation rate of PTEs differently in willow leaves when compared to the control sample. It was supposed that WA reduces the accumulation of PTEs in willows when applied together with MSSC and MSS, and the changed rate of PTE accumulation will affect the microanatomical parameters in the leaves of willows.

2. Materials and Methods

2.1. Long-Term Open-Field Experiment with Willow

The open-field small-plot long-term experiment was set up with energy willow in 2011 [2,17,44]. The research area was located parallel to Westsik Street in Nyíregyháza (Hungary, Europe) in the experimental field of the Research Institute of Nyíregyháza, University of Debrecen, Centre of Agricultural Sciences. Research plots were located at a height of 103.4 m above Baltic sea level, and are delimited with geographical coordinates 47°58′42.48059″ N, 21°41′58.96964″ E; 47°58′40.72898″ N, 21°41′59.04370″ E; 47°58′42.59343″ N, 21°42′02.34824″ E; and 47°58′40.87105″ N, 21°42′02.46138″ E. The total area of the long-term experiment was 3800 m^2. The experiment was set up with a randomized block design with ten various soil treatments in four replications (Figure S1), and hence there were 40 small plots [2,17,44].

In April 2011, before the first soil treatments, soil samples were taken from the experimental field from depths of 0–25 cm. The basic characteristics of the uncontaminated Cambisol (brown forest soil with clay stripes) with a loamy sand texture are indicated in Table 1 [44]. Element concentrations were determined in cc. HNO_3 − cc. H_2O_2 extracts followed the instructions of a Hungarian Standard MSZ 21470-50 2006 [45]. The experimental soil was considered uncontaminated with PTEs since PTE concentrations measured in the soil of experimental plots (Table 1) were definitively lower than the valid Hungarian threshold limits (As—15, Ba—250, Cd—1, Cr—75, Cu—75, Ni—40, Pb—100, and Zn—200 mg kg^{-1}) for soil pollution [46].

Willows (*Salix triandra* × *S. viminalis* 'Inger') were planted in April 2011; cuttings originated from Holland-Alma Ltd., Piricse, Hungary (the license holder of the studied willow species is Lantmännen Agroenergi AB, Sweden). In one 27 m^2 experimental plot, 40 willow bushes were grown with 0.75 m line spacing and 0.6 m between plants. In every small plot, plants were grown in two twin rows with 1.5 m spacing [2,17].

The long-term experiment ran from 2011 to 2021 and the period of soil treatments (Figures S1 and S2) was between April 2011 and June 2018. The top 0–25 cm layer of the soil was treated in the spring (during April, May, and June) of 2011, 2013, and 2016 with municipal sewage sludge compost (MSSC), willow ash (WA), and a combination of the two (MSSC + WA) (Figure S2), with 4 replications [44].

Municipal sewage sludge compost (producer Nyírségvíz Ltd., Nyíregyháza, Hungary) was applied to the topsoil at a dose of 15 t ha^{-1} (wet weight with 48–56% dry matter) each year [17]. Its PTE concentrations during 2016 in cc. HNO_3 − cc. H_2O_2 extracts are indicated in Table 1. The concentrations of PTEs in MSSC applied in 2011 and 2013 were in a similar range [44]. Other basic physical and chemical characteristics, as well as the plant nutrient content of MSSC [44], can be found in Table 1.

Table 1. Basic characteristics of the experimental soil [44] and additives applied to the soil [2,17,44] (open-field long-term experiment with energy willows, Nyíregyháza, Hungary).

Parameter	Soil (2011)	MSSC (2016)	WA (2016)	MSS (2018)	WA (2018)
pH-H_2O	8.10	5.93	10.9	7.11	-
pH-KCl	7.52	5.91	10.7	-	-
Total salt (m m^{-1} %)	<0.02	3.34	1.17	-	-
Water-soluble salt content (m m^{-1} %)	-	-	-	1.80	-
$CaCO_3$ (m m^{-1} %)	4.80	0	-	-	-
CEC (cmolc kg^{-1})	10.4	-	-	-	-
Humus (m m^{-1} %)	1.51	-	-	-	-
Total C (m m^{-1} %)	-	10.4	-	-	-
Total N (m m^{-1} %)	-	1.84	-	12,371	-
NH_4-N (mg kg^{-1})	-	169	0	357	-
NO_3-N (mg kg^{-1})	-	42.3	0	34.4	-
P (mg kg^{-1})	621	18,876	6472	4695	25,403
K (mg kg^{-1})	2918	3424	16,508	3077	54,248
Ca (mg kg^{-1})	16,307	39,294	43,074	34,724	187,550
Mg (mg kg^{-1})	4603	4479	7991	7049	35,348
As (mg kg^{-1})	9.60	12.2	10.2	31.0	18.5
Ba (mg kg^{-1})	57.5	212	267	596	403
Cd (mg kg^{-1})	0.21	0.55	2.38	1.23	0.60
Cr (mg kg^{-1})	13.7	19.3	9.66	1142	9.10
Cu (mg kg^{-1})	9.18	79.0	133	198	130
Mn (mg kg^{-1})	372	318	553	520	670
Ni (mg kg^{-1})	14.0	15.1	10.9	62.8	14.2
Pb (mg kg^{-1})	9.89	22.0	12.1	278	26.7
Zn (mg kg^{-1})	35.5	357	1757	978	1853

MSSC = municipal sewage sludge compost. MSS = municipal sewage sediment. WA = willow ash.

Willow ash was prepared by burning the leafless twigs of the willows, grown formerly in the experimental plots [17]. Willow ash (with 99% dry matter) was applied to the topsoil in 2011 and 2013 at a dose of 600 kg ha^{-1}, and at a dose of 300 kg ha^{-1} in 2016 [17,44]. PTE concentrations measured during 2016 in cc. HNO_3 − cc. H_2O_2 extract are indicated in Table 1. Concentrations of PTEs in applied WA in 2011 and 2013 were in a similar range [44]. The basic characteristics of the WA can be found in Table 1.

In June 2018, the soil of plots formerly treated with MSSC was amended with municipal sewage sediment (MSS) at a dose of 7.5 t ha^{-1} dose with 92% dry matter (Figure S2). At the same time, the soil was treated with WA for the fourth time at a dose of 300 kg ha^{-1} [2,17]. Municipal sewage sediment and WA were also applied to the soil in combination. All 2018 treatments were performed with 4 replications (Figure S2). Control plots remained untreated since 2011.

The municipal sewage sediment originated from the Lovász-zug suburban area of Debrecen, Hungary (47°29′07″ N, 21°35′46″ E), where a sewage settling pond was formerly operated as a secondary biological purification unit [21]. The former sampling and chemical analysis of MSS in studies [2,17] revealed that this wastewater solid is contaminated with PTEs (Table 1) [2,17]. Chemical analysis of MSS revealed that this wastewater solid is rich in calcium (Ca), magnesium (Mg), phosphorus (P), and potassium (K) [2]. The basic characteristics of the MSS can be found in Table 1 (unpublished results).

The PTE concentrations in WA during 2018 are indicated in Table 1. The WA contained considerable amounts of K, Ca, Mg, and P [2] (Table 1).

2.2. Soil Sampling

To check the impacts of the 3 applications (2011, 2013, and 2016) of MSSC, WA, or MSSC + WA on the concentrations of PTEs in soil, samples were taken on the 7th of June 2018 from 16 experimental plots, including controls. Approximately 1.2–1.5 kg of composite soil samples per plot were collected, drilling 10 cm away from the stems of 25 willow bushes. Twenty-five subsamples per plot were taken from a depth of 0–25 cm using a standard gouge auger (Royal Eikelkamp, Giesbeek, The Netherlands). All 16 plots included in this experiment were sampled using this method. Soil sampling was performed in 4 replicates per treatment. Soil sampling was repeated on 25 September 2020, from a depth of 0–30 cm, as described above. All soil sampling was performed in 4 replicates per treatment [2,17].

Immediately after sampling, all soil samples were taken to the laboratory. After the removal of foreign substances, the soil was homogenized and spread on plastic plates in a thin layer. After 14 days of drying at room temperature, the thoroughly mixed air-dried samples were passed through a 2 mm sieve [17].

2.3. Plant Sampling

The presented sampling of willow leaves was conducted on 24 June 2019; 53 weeks after the last soil treatments. Willow leaves were sampled from 10 plants per experimental plot. Five individuals of the sampled plants were located in the middle section of the 2nd row, while the other five were from the middle section of the 3rd row of a given plot. Ten fully developed leaves per plant were collected from the 10–20 cm uppermost section of the shoots. From each plot, 100 leaves were collected, as were 400 leaves from each treatment, with an average total fresh weight of 46 g per plot. All 16 plots included in the experiment were sampled in this way. Plant sampling was performed in 4 replicates per treatment [17].

Immediately after sampling, leaves were thoroughly washed in flowing tap water in the laboratory. The tap water was rinsed from the samples in distilled water that was changed twice. Samples were dried until constant loss of weight in a drying oven (Mytron, Mytron Bio- und Solartechnik GmbHd., Heilbad Heiligenstadt, Germany) at 70 °C for 10 h. Dry samples were ground to particles < 1 mm in size in an ultra-centrifugal mill (Retsch ZEM 200, Retsch Ltd., Haan NRW, Germany) [17].

The leaf samples for the microanatomical examinations were collected on 24 June 2019. For the examinations, intact, healthy, well-developed 5th-position leaves were collected. Five leaves were collected from each of the sampling blocks, thus 20 leaves were collected altogether. The collected leaves were preserved in Strasburger–Flemming's preservative solution (a mixture of 96% ethanol, 99.5% glycerol, and distilled water, in a 1:1:1 $v\ v^{-1}$ ratio) [47], until sectioning and preparation of the epidermis imprints.

2.4. Element Analysis of Soil and Plant Samples

To determine the "pseudo-total" element content of the soil, the Hungarian Standard MSZ 21470-50 2006 [45] was followed with slight modifications. The sample preparation procedure and the microwave digestion of 0.5 g of soil (<0.1 mm) in cc. HNO_3 and in cc. H_2O_2 (3:1 $v\ v^{-1}$) solutions are described in detail elsewhere [2,17,48].

From the prepared (dried and ground to particles < 0.1 mm in size) plant samples, 0.5 g was loaded into the pressure-proof bombs of the microwave digester (Milestone Ethos Plus, Sorisole (BG), Italy). Five mL of distilled cc. HNO_3 and 3 mL 30% ($v\ v^{-1}$) H_2O_2 (Scharlau, Barcelona, Spain) were added to all samples [17,48].

Elemental analysis of all soil or plant samples was conducted with the Inductively Coupled Plasma-Optical Emission Spectrometry (ICP-OES) technique, applied on an iCAP 7000 spectrophotometer (Thermo Fisher Scientific, Waltham, MA, USA). For the calibration, a multielement standard solution (n = 2) was applied. All element analyses were performed with 4 replicates [48].

2.5. Microanatomical Investigations of Leaves

Epidermis imprints and cross-sections were made from leaf samples following the methods of Hilu and Randall [49], Gardner et al. [50], and Elagöz et al. [51]. Imprints were made from the adaxial and abaxial surfaces of leaves, using clear nail polish. The imprint could be used as a negative to assess stomata density [52]. After drying the nail polish, imprints were examined under a BX51-type Olympus light microscope (Olympus BioSystems, Munich, Germany) [53,54]. In addition, the method of García-Gutiérrez et al. [55] was used: leaf segments were partially digested with Franklin's solution (a mixture of 35% hydrogen peroxide and glacial acetic acid in a 1:1 $v\ v^{-1}$ ratio) at room temperature for 24 h. This solution digests the parenchyma tissue, leaving the epidermis and leaf veins intact. After washing with water, leaf samples were placed in a solution of sodium hypochlorite (25–50% in water) to make the epidermis transparent. Next, the samples were washed with water to remove Franklin's solution and sodium hypochlorite. Finally, the samples were stained with a 0.01% safranin aqueous solution (Merck KGaA, Darmstadt, Germany). The following micromorphometric parameters were examined: stomatal density (frequency of stomatal complexes (no./mm^2)), width of stomatal complexes (µm), and length of stomatal complexes (µm).

Leaf cross sections were incised from the middle third part of the leaves using razor blades following the method of Sass [56]. Examination of the cross-sections was achieved by using the microscope mentioned above. Preparations were colored with a 0.01% aqueous solution of safranin (Merck KGaA, Darmstadt, Germany). The following micromorphometric parameters were examined: lamina thickness (µm), mesophyll thickness (µm), the adaxial epidermis (µm), the abaxial epidermis (µm), the adaxial cuticle (µm), the abaxial cuticle (µm), palisade mesophyll (µm), spongy mesophyll (µm), midrib height (µm), midrib width (µm), midrib extent (µm^2), vascular bundle height (µm), vascular bundle width (µm), vascular bundle extent (µm^2), adaxial sclerenchyma thickness (µm), abaxial sclerenchyma thickness (µm), adaxial collenchyma thickness (µm), and abaxial collenchyma thickness (µm).

A VSI RZ302 3M CMOS camera (Beijing BestScope Technology Co., Beijing, China) was used to prepare digital recordings, and a VSI RZ302 measuring program was applied to measure the above-mentioned micromorphometric parameters. The examined micromorphometric parameters on the cross-sections and epidermal imprints were measured and digitally archived at 4 × 10, 10 × 10, 20 × 10, and 40 × 10 magnifications. All investigated parameters were measured on 10 leaves per treatment, and the obtained data were averaged.

2.6. Statistical Analysis of Data

The test of normality of the data was performed with the Kolmogorov–Smirnov test ("Quest Graph™ Kolmogorov-Smirnov (K-S) Test Calculator." AAT Bioquest, Inc., (Pleasanton, CA, USA) https://www.aatbio.com/tools/kolmogorov-smirnov-k-s-test-calculator, accessed on 17 July 2024). The data of concentrations of potentially toxic elements (PTEs) in the leaves of energy willow (*Salix triandra* × *Salix viminalis* 'Inger') and their microanatomical parameters are normally distributed (Tables S1 and S2). Correlation coefficients (r) between concentrations of potentially toxic elements in leaves of energy willow and microanatomical parameters were calculated according to the correlation analysis formula used by Microsoft Excel 2016 ($p < 0.05$) (Table S3). To describe the relationship between the PTE concentrations and examined microanatomical parameters, linear regression analysis was performed using the regression analysis formula in Microsoft Excel 2016. Statistical analysis of experimental data was conducted with IBM SPSS Statistics 26.0 software using Analysis of Variance (ANOVA) followed by treatment comparison using Tukey's b-test.

3. Results and Discussion

3.1. PTEs in Experimental Soil

The soil in the experimental plots of the willows was treated with MSSC, WA, or MSSC + WA during 2011, 2013, and 2016. In addition to the beneficial mineral nutrients that could be utilized by the plants, the thrice-applied MSSC and WA also contained PTEs [2,17]. It was therefore assumed that surpluses of PTEs would be measurable in the topsoil of the experimental plots. To prove this, plots were first sampled in June 2018 to measure the concentrations of nine selected PTEs in the upper layer of the experimental soils (Table 2).

Table 2. Concentrations of PTEs in the topsoil of the open-field long-term experiment set up with energy willows (*Salix triandra* × *Salix viminalis* 'Inger'), Nyíregyháza, Hungary [17].

PTE * mg kg^{-1}	Soil Treatments (2011, 2013, and 2016)			
	Control	**MSSC**	**WA**	**MSSC + WA**
	Soil depth 0–25 cm (sampling June 2018)			
As	8.45 ^{a}	22.3 ^{d}	13.4 ^{b}	19.8 ^{c}
Ba	97.8 ^{a}	130 ^{c}	117 ^{b}	127 ^{c}
Cd	0.291 ^{a}	0.805 ^{d}	0.470 ^{b}	0.642 ^{c}
Cr	9.51 ^{a}	18.0 ^{c}	9.58 ^{a}	12.0 ^{b}
Cu	11.3 ^{a}	15.5 ^{d}	12.4 ^{b}	13.7 ^{c}
Mn	263 ^{a}	429 ^{b}	481 ^{d}	454 ^{c}
Ni	11.3 ^{a}	14.9 ^{d}	12.6 ^{b}	13.9 ^{c}
Pb	15.4 ^{a}	35.3 ^{d}	16.6 ^{b}	23.1 ^{c}
Zn	40.3 ^{a}	51.4 ^{b}	55.6 ^{d}	54.0 ^{c}
	Soil Treatment (2018)			
	Control	**MSS**	**WA**	**MSS + WA**
	Soil depth 0–30 cm (sampling September 2020)			
As	9.19 ^{a}	35.6 ^{d}	27.3 ^{b}	30.4 ^{c}
Ba	56.0 ^{a}	67.3 ^{d}	59.6 ^{b}	63.5 ^{c}
Cd	0.214 ^{a}	0.625 ^{d}	0.391 ^{b}	0.494 ^{c}
Cr	12.6 ^{a}	17.5 ^{c}	13.1 ^{a}	15.8 ^{b}
Cu	9.47 ^{a}	12.0 ^{d}	10.1 ^{b}	11.2 ^{c}
Mn	368 ^{a}	482 ^{b}	529 ^{b}	500 ^{b}
Ni	13.5 ^{a}	14.1 ^{b}	14.9 ^{c}	14.7 ^{c}
Pb	10.1 ^{a}	13.7 ^{d}	11.4 ^{b}	12.4 ^{c}
Zn	35.3 ^{a}	40.2 ^{b}	43.2 ^{b}	41.9 ^{b}

* PTE = potentially toxic elements measured in cc. HNO_3 + cc. H_2O_2 extract. MSSC = municipal sewage sludge compost. MSS = municipal sewage sediment. WA = willow ash. The data were evaluated by one-way ANOVA followed by Tukey's b-test at 0.05 to determine significant differences indicated by different letters (n = 4).

All treatments significantly ($p < 0.05$) increased the concentrations of all PTEs in soils compared to the control (Table 2). The only exception was Cr in WA-treated soil (Table 2). The highest As, Ba, Cd, Cu, Cr, Ni, and Pb concentrations were detected in MSSC-treated soil, while the most elevated Mn and Zn contents were present in WA-treated soil. This was related to significant amounts of Mn and Zn present in willow ash [44]. Except for Mn and Zn, the co-application of MSSC and WA resulted in significantly lower PTE concentrations in soil compared to the application of MSSC alone.

In June 2018, the soil of plots formerly treated three times with MSSC was amended with MSS. WA was applied a fourth time to the soil. The second soil sampling for PTE concentration analysis was conducted in September 2020, which was 116 weeks after the last soil treatments in June 2018. The measured PTE concentrations in the upper soil are also presented in Table 2.

The results of this study confirm the well-known phenomenon that single or repeated application and long-term soil disposal of municipal sewage sludge or wood ash can considerably increase the concentrations of PTEs in topsoil [3,5,9]. The PTE concentrations measured in the soils of experimental plots in this study remained lower than the valid Hungarian threshold limits (As—15, Ba—250, Cd—1, Cr—75, Cu—75, Ni—40, Pb—100, and Zn—200 mg kg^{-1}) for soil pollution [46].

The results from 2020 confirm observations from 2018 (Table 1), namely that all soil additives significantly increased the concentrations of the studied group of PTEs in topsoil, as compared to the untreated control. Similarly to 2018, it was recognized that co-application of MSSC + MSS and WA resulted in significantly lower As, Ba, Cd, Cr, Cu, and Pb concentrations in topsoil than the application of MSSC + MSS alone (Table 2) [2].

During September 2020, in the 0–30 cm layer of soil treated with MSSC + MSS, WA, or MSSC + MSS + WA, 197–287% more As, 6–20% more Ba, 83–192% more Cd, 4–39% more Cr, 7–27% more Cu, 31–44% more Mn, 4–10% more Ni, 13–36% more Pb, and 14–22% more Zn were detected in HNO_3–H_2O_2 extracts (Table 2), as compared to PTE concentrations in untreated control soil [2].

It was assumed that the enhanced concentration of PTEs in soil will alter the element composition of the willow leaves and this will affect the microanatomical parameters.

3.2. PTEs in Willow Leaves

Table 3 presents the effects of various soil treatments on the concentrations of PTEs in the leaves of energy willows during June 2019.

Table 3. Concentrations of PTEs in the leaves of energy willows (*Salix triandra* × *Salix viminalis* 'Inger') affected by various soil treatments (long-term open-field experiment, Nyíregyháza, Hungary) [17].

PTE * ($\mu g\ g^{-1}$)	Soil Treatments (2011, 2013, 2016, and 2018)			
	Control	**MSSC + MSS**	**WA**	**MSSC + MSS + WA**
	Willow leaves (June 2019)			
As	0.176 ^{a}	0.295 ^{d}	0.200 ^{b}	0.243 ^{c}
Ba	4.66 ^{b}	4.22 ^{a}	6.89 ^{d}	5.47 ^{c}
Cd	0.847 ^{b}	0.913 ^{d}	0.792 ^{a}	0.883 ^{c}
Cr	0.266 ^{a}	0.543 ^{d}	0.348 ^{b}	0.461 ^{c}
Cu	8.04 ^{a}	8.99 ^{c}	8.40 ^{b}	8.54 ^{b}
Mn	35.8 ^{a}	34.3 ^{a}	41.1 ^{c}	37.9 ^{b}
Ni	1.06 ^{b}	1.57 ^{d}	0.97 ^{c}	1.21 ^{c}
Pb	0.097 ^{a}	0.308 ^{c}	0.114 ^{a}	0.220 ^{b}
Zn	79.7 ^{c}	67.9 ^{a}	79.9 ^{c}	73.0 ^{b}

* PTE = potentially toxic elements measured in cc. HNO_3 + cc. H_2O_2 extract. Soil treatments: MSSC = municipal sewage sludge compost, MSS = municipal sewage sediment, WA = willow ash. The data were evaluated by one-way ANOVA followed by Tukey's b-test at 0.05 to determine significant differences indicated by different letters (n = 4).

It can be generally declared that all former soil treatments significantly enhanced the uptake or accumulation of PTEs in the leaves of willows (Table 3), [2]. Elevated levels of As, Cd, Cr, Cu, Ni, and Pb in the leaves of willow are, however, in the normal range for plants [57,58].

During June 2019, 53 weeks after the last soil treatments, in the leaves of willows treated with MSSC + MSS, WA, or MSSC + MSS + WA, 14–68% more As, 17–48% more Ba, 31–104% more Cr, 4–12% more Cu, 6–15% more Mn, 18–218% more Pb, and 11–35% more Zn were detected, compared to the untreated control. In 2019, MSSC + MSS treatments significantly enhanced As, Cd, Cr, Cu, Ni, and Pb accumulation in leaves, while former WA treatments reduced Cd accumulation by 6,5% compared to the control.

Trace element concentrations in plants reflect, in most cases, their abundance in the growth media. Generally, Cr is very slightly soluble in the soil solution and is not easily taken up by plants; As and Pb are relatively strongly absorbed by soil particles and are not readily transported to the above-ground parts of plants; Cu, Mn, and Ni are mobile in soil and readily taken up by plants, while Cd and Zn are very mobile in soil, and are easily bioaccumulated by plants [57,58]. These general observations are largely supported by measured PTE concentrations in the leaves of willow (Table 3).

Salix spp. are well-known accumulators of Zn and Cd [9,14–16]. This was also supported by the results presented in Table 3. Zinc is taken up actively from the soil to aboveground plant organs, while Cd is accumulated passively [57,58]. Bioconcentration factor (BCF) can be calculated by dividing the concentration of a given PTE in leaves by the concentration of a given PTE in the soil. Bioconcentration factor ratios above 1 mean that the plant actively concentrates the metal in its tissues [9,16]. Bioconcentration factors varied from 1.79 to 3.95 for cadmium, and from 1.69 to 2.25 for zinc (presented in Tables 2 and 3).

3.3. General Microanatomical Characteristics of the Leaf Blade

The leaves of the energy willow are dorsiventral and mainly hyposomatic, the same as those of other species from the Caprisalix subgenus [28]. However, if the root/shoot ratio is high, they can also be amphistomatic. Therefore, the leaves are, at the beginning of their development (leaf area < 2.8 cm^2) or with outstanding water supply, amphistomatic. However, in the case of fully developed leaves, especially in the case of those exposed to abiotic stress, the stomata on the adaxial side of the leaves may close. In this case, the adaxial epidermis can be observed with stomatal occlusions and no active stomata (Figure 1). This strategy can limit water loss during leaf development, as mature leaves can adapt to the abiotic conditions of the given place of production [59–61]. On the abaxial side, stomata can be found in-between polygonal epidermal cells with wavy walls. The stomata are paracytic and are bordered by two guard cells, which have longitudinal axes parallel to the stomatal subsidiary cell. The position of the stomata is random. The adaxial and abaxial epidermis are covered in a thin cuticle layer. The leaves are covered in non-glandular trichomes which are mostly unicellular, long-covered hairs with thin walls.

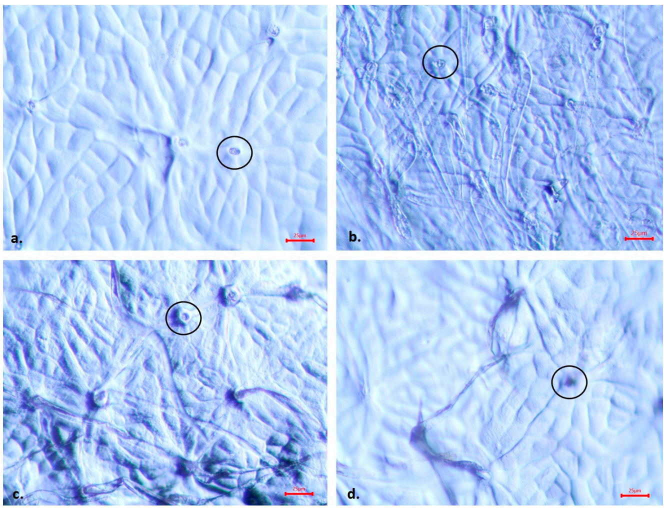

Figure 1. Microscopic images of the adaxial faces of mature *Salix triandra* × *S. viminalis* 'Inger' leaves illustrating stomatal occlusions (black circles) (**a**) Control (20×), (**b**) WA (20×), (**c**) MSSC + MSS (20×), (**d**) MSSC + MSS + WA (20×). WA = wood ash. MSSC = municipal sewage sludge compost. MSS = municipal sewage sediment. Scale bars: 25 µm.

The mesophyll is built of palisade (two or three cell rows) and spongy parenchyma (three cell rows). The mesophyll cells sit close to each other, and between the spongy parenchyma cells, some airspace (directly above the stomata) can be found. The presence of rosette Ca-oxalate crystals is a typical characteristic of the leaf mesophyll. In the mesophyll cells surrounding the midrib, Ca-oxalate pyramids and crystal sand are typical as a vacuole-filling component. The idioblast cells can be observed mostly in-between the mesophyll cells close to the midrib, while a small amount of these cells are further away from the midrib, mainly in the spongy parenchyma. The idioblast cells showed characteristic differences in shape and size compared to the mesophyll cells [54] (Figure 2).

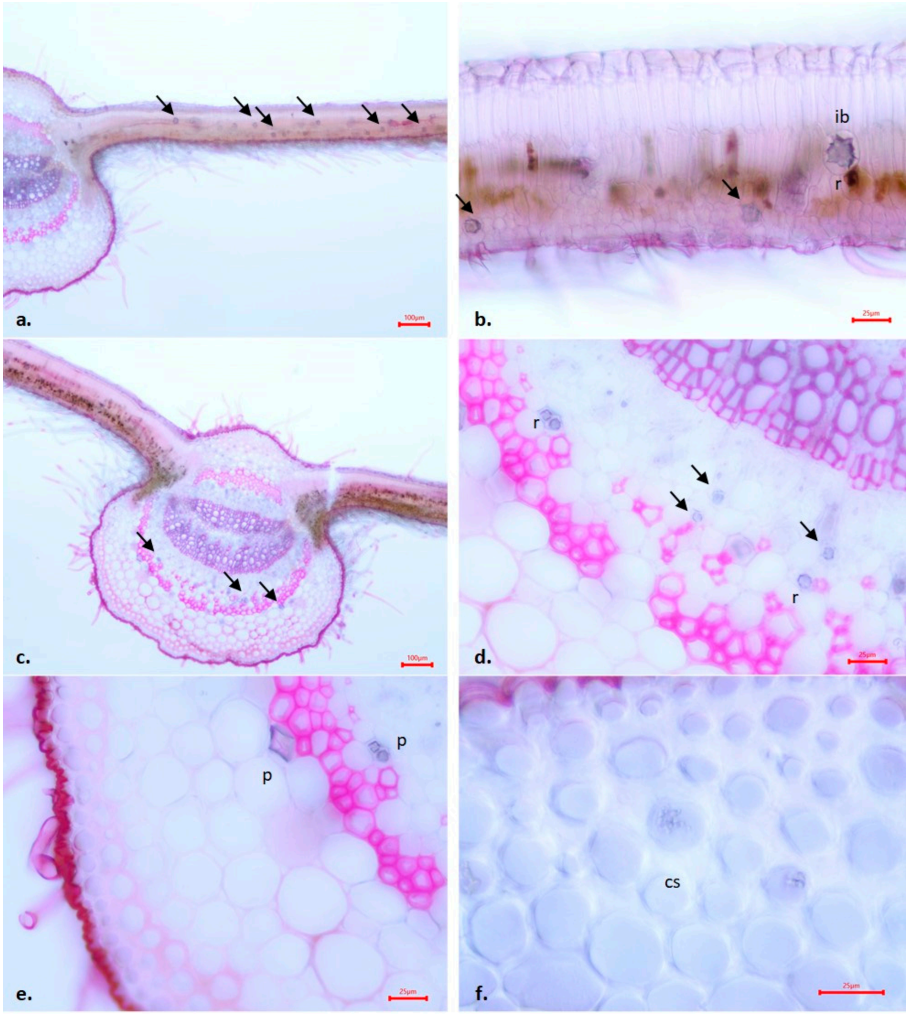

Figure 2. Transverse section of leaf laminas of *Salix triandra* × *S. viminalis* 'Inger'. Different types of Ca-oxalate crystals: Ca-oxalate crystal rosette (r) is a typical characteristic of the leaf mesophyll but can also be found in the mesophyll cells of the midrib area (black arrows). Surrounding the midrib are the Ca-oxalate pyramids (p) and crystal sand (cs). The idioblast cells (ib) can be typical in the leaf mesophyll. (**a**) Cross-section of the leaf—WA (4×), (**b**) leaf mesophyll—Control (20×), (**c**) cross-section of the leaf—Control (4×), (**d**) Ca-oxalate crystal rosettes in the midrib of mesophyll cells—Control (20×), (**e**) Ca-oxalate pyramids in the midrib of mesophyll cells—Control (20×), (**f**) Crystal sand in the midrib of mesophyll cells—Control (40×). WA = wood ash. Scale bars: (**a**) 100 µm, (**b**) 25 µm, (**c**) 100 µm, (**d**) 25 µm, (**e**) 25 µm, (**f**) 25 µm.

3.4. Characteristic Alterations in the Microanatomical Properties of the Leaf

Due to the nature of the materials used in the different treatments in the experimental area, (i.e., MSSC, the applied MSS, and the applied WA), they contained PTEs as well as nutrient elements [17]. This was also confirmed by the following observations: in 2019, MSSC + MSS treatments significantly increased As, Cd, Cr, Cu, Ni, and Pb accumulation in leaves, while former WA treatments reduced Cd accumulation by 6.5%, as compared to the control. In 2019, the effects of soil treatments on the concentrations of PTEs in the leaves of energy willows (*Salix triandra* × *Salix viminalis* 'Inger') were formed as follows in the MSSC + MSS treatment: As: 0.295 mg kg^{-1}, Cd: 0.913 mg kg^{-1}, Cr: 0.543 mg kg^{-1}, Cu: 8.99 mg kg^{-1}, Ni: 1.57 mg kg^{-1}, and Pb: 0.308 mg kg^{-1} (Table 3) [2]. The concentrations of these PTEs were significantly higher than in the case of the control and other treatments. In the case of other treatments (WA and MSSC + MS + WA), the concentrations of Ba, Mn, and Zn were significantly higher than in the case of MSSC treatment. Based on the above, it was hypothesized that the altered element composition of the leaves affected the microanatomical parameters.

The thickness of the leaf lamina was the lowest in the case of MSSC + MSS treatment, and this significant ($p < 0.05$) difference was statistically proven compared to the other treatments (Table 4). For samples from this treatment, the extent of the leaf plate decreased by 32.5% compared to the control. In the case of the other two treatments, the volume of the reducing effect of the treatment was smaller (in the case of WA treatment, the leaf lamina decreased by 20%, in the case of MSSC + MSS + WA, it decreased by 28%), but it was also statistically significant. The application of WA reduced the negative effects of the MSS on the extent of the leaf lamina. Similarly to the observation above, the extent of the leaf mesophyll was statistically proven to be the smallest in the case of MSSC + MSS treatment. Compared to the values measured in the control samples, the extent of the leaf mesophyll decreased by 30% due to this treatment. However, the WA treatment caused a decrease of only 22%, and the MSSC + MSS + WA treatment caused a 26% reduction in the size of the mesophyll compared to the control. In the case of this last treatment, the addition of the WA to the MSSC + MSS treatment had a mitigating influence on the negative effects MSSC + MSS treatment alone.

Table 4. Effects of soil treatments on the anatomical characteristics of the leaves of energy willows (*Salix triandra* × *Salix viminalis* 'Inger'), grown in a long-term open-field experiment (Nyíregyháza, Hungary).

	Control	MSSC + MSS	WA	MSSC + MSS + WA
Lamina thickness (μm)	160.37 ± 4.41 ^{d}	108.3 ± 2.17 ^{a}	129.14 ± 1.63 ^{c}	115.93 ± 2.25 ^{b}
Mesophyll thickness (μm)	138.54 ± 3.031 ^{d}	89.01 ± 1.14 ^{a}	108.58 ± 1.21 ^{c}	102.62 ± 1.69 ^{b}
Adaxial epidermis (μm)	8.62 ± 0.36 ^{c}	6.43 ± 0.52 ^{a}	7.53 ± 0.23 ^{b}	10.27 ± 0.55 ^{d}
Abaxial epidermis (μm)	7.73 ± 0.45 ^{d}	5.82 ± 0.53 ^{c}	4.07 ± 0.24 ^{b}	3.24 ± 0.46 ^{a}
Adaxial cuticule (μm)	2.67 ± 0.23 ^{c}	1.67 ± 0.30 ^{a}	2.11 ± 0.03 ^{b}	1.60 ± 0.05 ^{a}
Abaxial cuticule (μm)	2.53 ± 0.16 ^{d}	0.79 ± 0.18 ^{a}	2.01 ± 0.07 ^{c}	1.07.06 ^{b}
Palisade mesophyll (μm)	108.34 ± 4.17 ^{c}	62.27 ± 1.96 ^{a}	72.12 ± 2.99 ^{b}	71.75 ± 3.33 ^{b}
Spongy mesophyll (μm)	26.01 ± 1.98 ^{a}	25.49 ± 1.76 ^{a}	35.76 ± 3.13 ^{b}	47.19 ± 1.53 ^{c}
Midrib height (μm)	904.82 ± 2.91 ^{d}	775.11 ± 11.88 ^{a}	828.3 ± 3.30 ^{b}	883.40 ± 7.76 ^{c}
Midrib width (μm)	952.26 ± 0.71 ^{b}	893.31 ± 4.39 ^{a}	995.60 ± 9.85 ^{c}	1032.01 ± 15.53 ^{d}
Midrib extent (μm^2)	632,852.38 ± 87.47 ^{c}	514,054.48 ± 40.88 ^{a}	599,965.83 ± 103.18 ^{b}	638,752.14 ± 66.71 ^{d}
Vascular bundle height (μm)	402.85 ± 1.52 ^{d}	312.11 ± 1.99 ^{a}	364.26 ± 4.39 ^{b}	371.77 ± 2.12 ^{c}
Vascular bundle width (μm)	604.72 ± 1.47 ^{c}	546.06 ± 4.16 ^{a}	581.12 ± 1.57 ^{b}	578.88 ± 1.83 ^{b}
Vascular bundle extent (μm^2)	187,072.23 ± 34.89 ^{d}	153,676.29 ± 33.63 ^{a}	184,343.58 ± 226.64 ^{c}	17,7624.96 ± 35.36 ^{b}
Adaxial sclerenchyma thickness (μm)	16,465.33 ± 68.25 ^{d}	6812.55 ± 26.22 ^{a}	11,118.63 ± 18.76 ^{b}	11,379.74 ± 21.03 ^{c}
Abaxial sclerenchyma thickness (μm)	32,067.16 ± 24.33 ^{c}	3176.68 ± 11.40 ^{a}	16,218.54 ± 16.95 ^{b}	41,974.58 ± 54.26 ^{d}
Adaxial collenchyma thickness (μm)	26,203.77 ± 35.91 ^{c}	17,548.54 ± 11.64 ^{a}	17,832.75 ± 28.88 ^{b}	38,359.65 ± 30.90 ^{d}
Abaxial collenchyma thickness (μm)	67,517.32 ± 94.92 ^{b}	46,571.19 ± 19.62 ^{a}	53,397.95 ± 16.31 ^{b}	58,152.39 ± 35.01 ^{c}
Stomatal density (no./mm^2)	167.4 ± 3.20 ^{a}	327.9 ± 13.4 ^{d}	203.1 ± 6.45 ^{b}	222.4 ± 6.47 ^{c}
Width of stomatal complexes (μm)	18.59 ± 0.1 ^{d}	12.25 ± 0.25 ^{a}	15.48 ± 0.09 ^{c}	14.25 ± 0.13 ^{b}
Length of stomatal complexes (μm)	28.25 ± 0.18 ^{cd}	21.91 ± 0.89 ^{a}	27.78 ± 0.25 ^{c}	24.87 ± 0.47 ^{b}

MSSC = municipal sewage sludge compost. MSS = municipal sewage sediment. WA = wood ash. Data are means of 10 replications. ANOVA Tukey's b-test. Means within the lines followed by the same letter are not statistically significant at $p < 0.05$.

These observations are in agreement with the results of Nikolic et al. [36], Di Baccio et al. [37], and Stoláriková–Vaculíková et al. [40]. Nikolic et al. [36] investigated the potential of *Populus* species for phytoextraction of Cd-contaminated soil. Poplar clones were analyzed for the growth response of the plant to Cd contamination and morphological, anatomical, and histological reactions to Cd stress, as a function of biomass production. They concluded that the accumulated PTEs have a large effect on the leaf lamina thickness, the mesophyll thickness, the midrib characteristics (area of the vascular bundle and vessel lumen area), the area of spongy tissue, and the thickness of the abaxial epidermis. The results of Di Baccio et al. [37] showed that Zn treatments induced variations in leaf mesophyll thickness, intercellular spaces, and stomatal density and size. In the case of the willow hybrid that was examined in this study, it was observed that out of the PTEs accumulated in the leaf, Cd did not have a significantly negative effect on the development of the thickness of the leaf lamina and leaf mesophyll. The present examination shows that the increase in Cr concentration has a strong negative correlation with the evolution of the extent of both the leaf lamina ($r = -0.9188$) and leaf mesophyll ($r = -0.9262$). As a result of the regression analysis, it can be concluded that within the examined Cr concentration range, a 0.1 mg/kg change in the concentration of Cr causes a decrease of 18.276 µm in the thickness of leaf lamina and a decrease of 15.671 in the thickness of leaf mesophyll. Out of the accumulated PTEs, As ($r = -0.8713$), Cu ($r = -0.8736$), and Pb ($r = -0.8286$) had a significantly negative effect on the development of the leaf lamina thickness. The concentration of these elements within the leaf also has a strong negative correlation with the change in the thickness of the leaf mesophyll (As: $r = -0.8956$; Cu: $r = -0.8828$; Pb: $r = -0.8465$) (Figure 3a,b).

Palisade mesophyll in examined *Salix* spp. leaves were built from two- or three-celled layers. The cells were tightly connected, and between them, no intercellular spaces could be observed. The cells were elongated in shape and contained numerous elliptical-shaped chloroplasts. In the palisade mesophyll of the control leaf, there were three cell rows. In the two upper layers, the palisade cells were large, and the height of the cells in the bottom layer was short. Contrary to this, in the treated leaves, mainly in the leaves that originated from the MSSC + MSS-treated and MSSC + MSS + WA-treated plots, the palisade parenchyma was often formed by two cell layers. The spongy mesophyll consisted of three cell rows.

Inside the mesophyll, the extent of the palisade mesophyll cells was strongly affected by all of the treatments. The palisade mesophyll thickness was the smallest under the MSSC + MSS treatment. Compared to the control, the extent of the palisade mesophyll decreased by 43%, and the difference was statistically proven. The difference was also statistically significant in the case of the other two treatments (WA and MSSC + MSS + WA); however, the reduction of the extent of the palisade mesophyll inside the leaf was smaller. Under the MSSC + MSS + WA treatment, the extent of the palisade mesophyll was significantly higher (7%) than under the MSSC + MSS treatment.

The extent of the spongy mesophyll developed in a specific way as a result of each treatment: while in the case of the samples from the MSSC + MSS treatment, there was no difference in the microanatomical parameters compared to the control samples, in the case of samples from the WA and MSSC + MSS + WA treatments, the extent was statistically proven to be bigger (37% and 81%) compared to the control samples. These results suggest that the WA has a positive effect on the extent of both the palisade and the spongy mesophyll, and can compensate for the negative histological effects of the PTEs.

The results of Krzesłowska et al. [62], who examined the anatomy and ultrastructure of the leaf blade of Norway maple (*Acer platanoides* L.) grown on mining sludge, are confirmed by the results of this study. Similarly to us, they concluded that the effects of the PTEs on the alterations in leaf anatomy predominantly consist of the following: a significant decrease in palisade mesophyll width; more compact leaf tissue organization; and significantly smaller cells in the palisade parenchyma. Several other studies [34,35,37,38,41–43] also confirm the results presented in this study, reporting a similar trend when examining the effect of PTEs on leaf mesophyll.

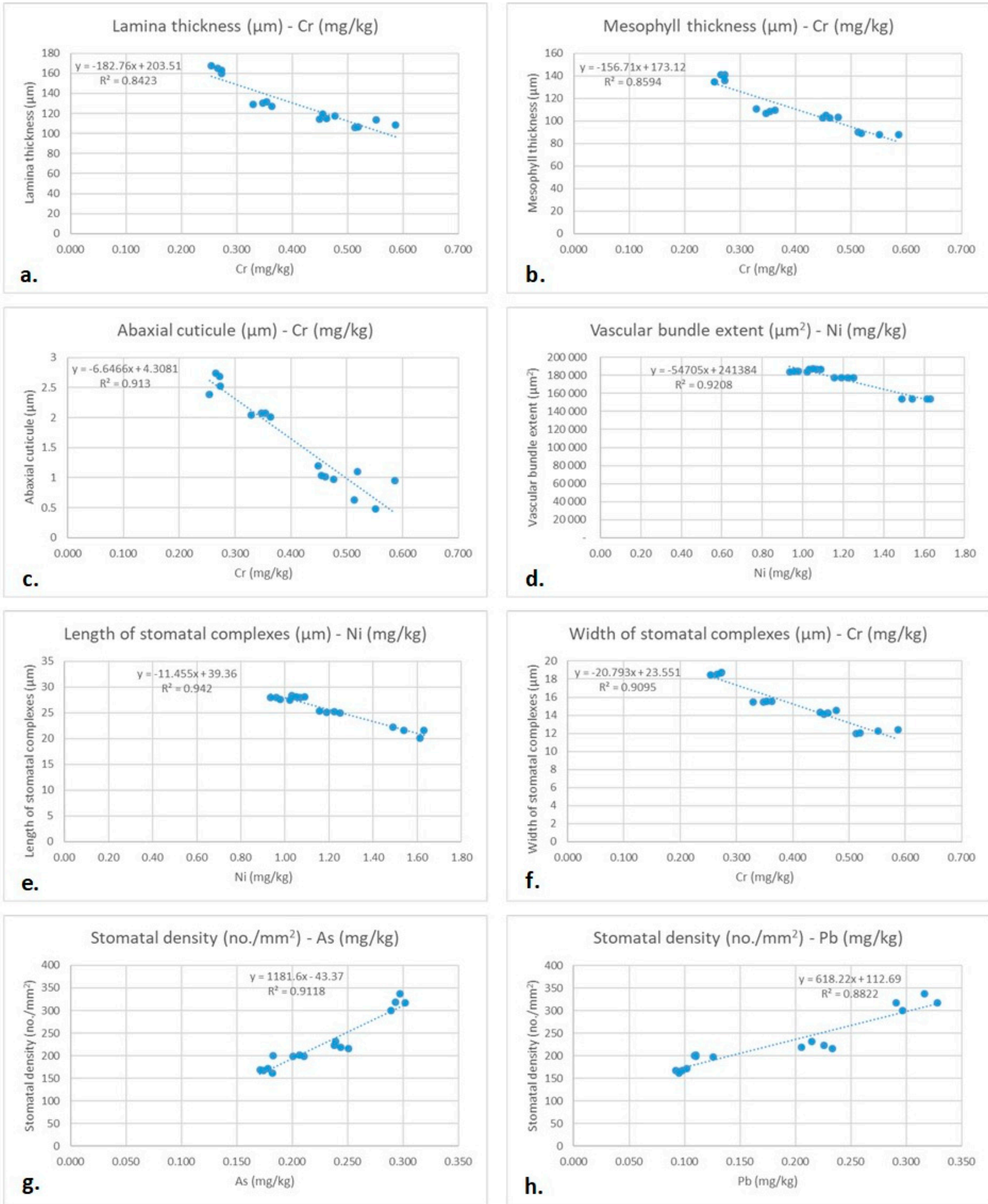

Figure 3. Linear regression analysis between PTE concentrations and micromorphological parameters. (the regression line, regression function, and the value of regression coefficient). (**a**) The relationship between Cr concentration (mg/kg) and lamina thickness (µm), (**b**) The relationship between Cr concentration (mg/kg) and mesophyll thickness (µm), (**c**) The relationship between Cr concentration (mg/kg) and abaxial cuticule thickness (µm), (**d**) The relationship between Ni concentration (mg/kg) and vascular bundle extent (µm^2), (**e**) The relationship between Ni concentration (mg/kg) and length of stomatal complexes (µm), (**f**) The relationship between Cr concentration (mg/kg) and width of stomatal complexes (µm), (**g**) The relationship between As concentration (mg/kg) and stomatal density (no./mm^2), (**h**) The relationship between Pb concentration (mg/kg) and stomatal density (no./mm^2).

The cells building the adaxial epidermis displayed a variability of shapes. In the control leaf, the cells appeared rectangular. In the MSSC + MSS-treated leaf, the cells were smaller and mainly oval, reduced and rectangularly shaped, or sometimes triangular. In the control leaf blade, the cells forming the abaxial epidermis were rectangularly shaped, and the longer axis of the cells was arranged parallel to the mesophyll of the leaf. They were relatively narrow. In the leaves from plants grown in the treated plots, the cells of the abaxial epidermis were also rectangular, and the longer axis of the cells was arranged perpendicularly to the leaf section. Sometimes, small triangular cells can be observed between the larger cells (Figure 4).

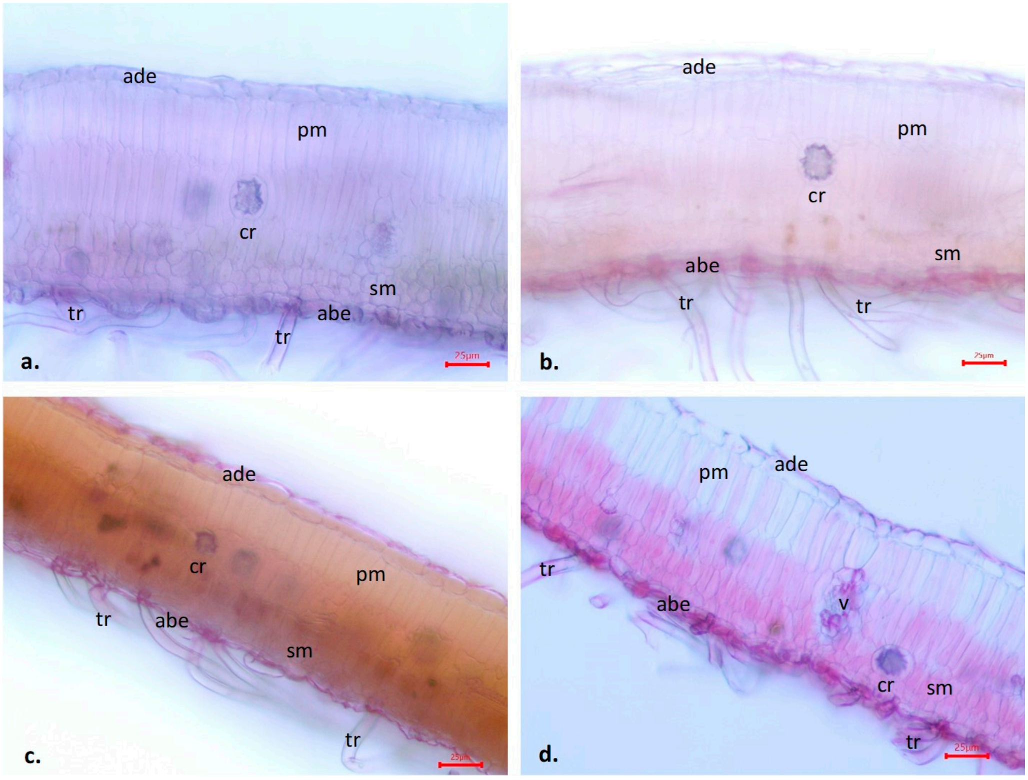

Figure 4. Transverse section of leaf laminas of *Salix triandra* × *S. viminalis* 'Inger'. Effects of soil treatments on the anatomical characteristics of the leaf lamina. (**a**) Control (20×), (**b**) WA (20×), (**c**) MSSC + MSS (20×), (**d**) MSSC + MSS + WA (20×). MSSC = municipal sewage sludge compost. MSS = municipal sewage sediment. WA = wood ash. ade: adaxial epidermis, abe: abaxial epidermis, pm: palisade mesophyll, sm: spongy mesophyll, v: vein, cr: Ca-oxalate crystal rosette, tr: trichomes. Scale bars: 25 µm.

Compared to the control, the MSSC + MSS treatment had a negative effect on the thickness of both the adaxial (25% reduction) and the abaxial epidermis (also 25% reduction), and this effect is statistically proven (Table 4). A significantly thinner epidermis was measured in the case of WA treatment compared to the control, but the reduction of the adaxial epidermis was significantly smaller compared to the MSSC + MSS treatment. In light of this, it is surprising that out of all treatments, the highest thickness of the epidermis was significantly observed in the case of MSSC + MSS + WA treatment. In this case, the thickness of the adaxial epidermis increased by 19% compared to the control. However, the thickness of the abaxial epidermis was the smallest in this treatment, and this result was significant. The thickness of the abaxial epidermis significantly decreased in the following order: control (7.73 µm), MSSC + MSS (5.82 µm), WA (4.07 µm), and MSSC + MSS + WA (3.24 µm). Similar to the results of this study, several studies [28,31–33,63] reported that the epidermal layer of the abaxial sides thickened with increasing PTE contamination.

The thickness of the adaxial cuticle was statistically proven to be smaller in the case of both MSSC + MSS treatments compared to the control (Table 4). With the MSSC + MSS treatment, the amount of the reduction was 37%, and in the MSSC + MSS + WA treatment, it was 40%. Although a significantly lower abaxial cuticle thickness was measured in the case of the WA treatment compared to the control, it was only reduced by 21%. However, in the case of WA treatment, an additional treatment was not able to mitigate the negative effects of the MSSC + MSS treatment on cuticle thickness. It could be determined by examining the thickness of the abaxial cuticle that every treatment affected it significantly and negatively. The MSSC + MSS treatment reduced the thickness of the abaxial cuticle to the greatest extent (the amount of the reduction was 79%). The WA treatment had fewer negative effects on the evolution of this parameter (it only caused a 21% reduction). In the case of the combined MSSC + MSS + WA treatment—probably due to the WA treatment—the reduction of the thickness of the abaxial cuticle (58%) did not reach the extent of the reduction observed in the case of leaves treated with only MSSC + MSS.

Both the adaxial and abaxial cuticle layers were the thinnest in the case of MSSC + MSS treatment. In the samples from this treatment, the Cr, As, and Pb concentrations of the leaves are two to three times higher compared to the concentration measured in control parcels, and significantly exceeded the concentration values measured in leaf samples from the other treatments (Table 2). Correlation analysis shows that out of the PTEs accumulated in the leaf, As (r = −0.9334), Cr (r = −0.9555), and Pb (r = −0.9281) had significantly negative effects on the development of the thickness of the abaxial cuticle. The result of the regression analysis highlights that in the examined Cr concentration range, a 0.1 mg/kg concentration change in Cr causes a decrease of 0.665 µm in the cuticle layer covering the abaxial leaf surface of the willow leaves (Figure 3c). The change in Cr concentration also showed a strong negative correlation with the thickness of the adaxial cuticle layer (r = −0.8388).

The significant decrease in the height of the midrib was observable in all of the treatments (Figure 5). In the case of this parameter, the most significant reduction (14%) was also caused by the MSSC + MSS treatment (Table 4). The WA treatment caused a lower volume of reduction, with only 8%. In the case of the MSSC + MSS + WA treatment, there was a 2% reduction. In the case of the evolution of this parameter, it can also be stated that the WA treatment reduced the degree of the decrease. In the evolution of the width of the midrib, a similar tendency is observable, and the differences between the treatments are minor. While the MSSC + MSS treatment significantly decreased the thickness of the midrib (6%), in the case of the two treatments with WA, the thickness of the midrib was significantly larger compared to the control and the MSSC + MSS treatment. Compared to the MSSC + MSS treatment, the MSSC + MSS + WA treatment increased the width of the midrib by 14%. This means that as a result of the treatments, the extent of the midrib was significantly smaller in the case of the MSSC + MSS treatment compared to the control (by 19%) and the MSSC + MSS + WA treatment (by 13%). Due to the WA treatment, the extent of the midrib was proven to be significantly smaller than the control. However, in the case of this treatment, the extent of the midrib was significantly larger thanks to the MSSC + MSS + WA treatment.

By examining the effects of the PTEs accumulated in the willow leaf on the size and extent of the midrib, it was observed that the concentrations of Cr, Pb, and Ni show a strong negative correlation with the change of this parameter. With the increase of their ratio within the leaf, the size of the midrib decreases. According to the results of this study, the values of the correlational coefficients were the following: Cr: r = −0.9502 (the concentration of Cr was 1.5–2 times higher compared to the values of samples from control parcels in all treatments (Table 2)), Pb: r = −0.9482 (the concentration of the samples from the treated parcels was 2–3 times higher compared to the control samples), Ni: r = −0.9595. The result of the regression analysis shows that in the examined Ni concentration range, a 0.1 mg/kg Ni concentration change causes a decrease in the extent of the midrib by 5470.5 μm^2 (Figure 3d).

The height and the width of the vascular bundles of the midrib did not reach the control values, and the differences were statistically proven (Table 4). The MSSC + MSS treatment reduced the above parameters to the greatest extent. In this case, the height of the vascular bundles decreased by 23% compared to the control, and the width decreased by 10%. In the case of the WA and MSSC + MSS + WA treatments, these parameters were significantly higher compared to the values measured by the MSSC + MSS treatment. WA treatment was able to positively influence the negative effects of MSSC + MSS treatment in the case of MSSC + MSS + WA treatment (in the case of the height, by 19%, and in the case of the width, by 6%). The extent of the vascular bundle was significantly smaller in every treatment compared to the control. In the case of the MSSC + MSS treatment, the reduction was the largest (by 18%). Compared to this, the extent of the vascular bundles increased significantly, by 15% in the treatment combined with WA. As in the case of most parameters, the smallest decrease compared to the control was observed for this parameter, and also in the case of the WA treatment (1.5% decrease) (Figures 6 and 7). The results of this study regarding the monitoring of changes in the extent of the middle ribs and vascular bundle are similar to the results of other studies [35,63].

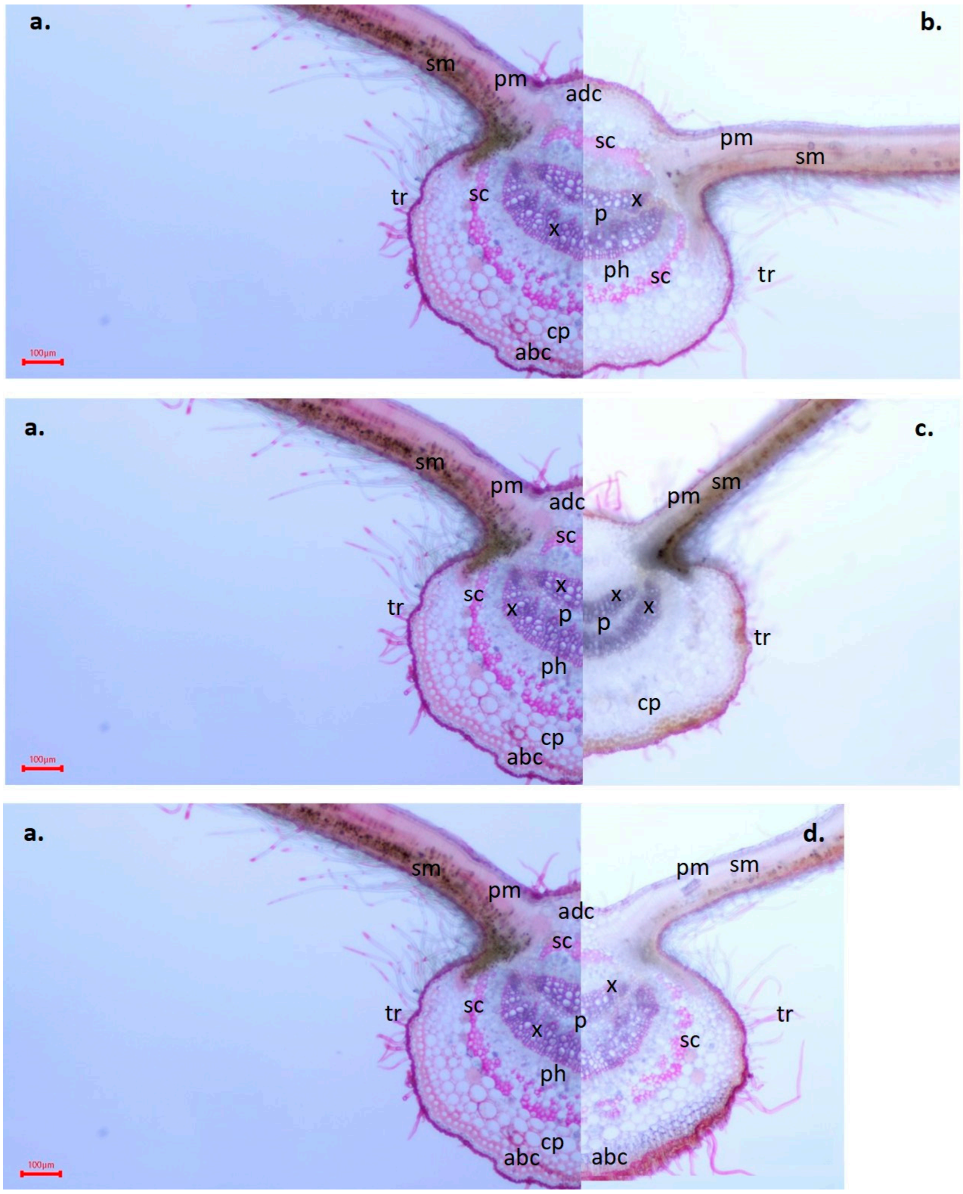

Figure 5. Transverse section of leaf laminas of *Salix triandra* × *S. viminalis* 'Inger'. Effects of soil treatments on the anatomical characteristics of the midrib I. (**a**) Control (4×), (**b**) WA (4×), (**c**) MSSC + MSS (4×), (**d**) MSSC + MSS + WA (4×). MSSC = municipal sewage sludge compost. MSS = municipal sewage sediment. WA = wood ash. adc: adaxial collenchyma, abc: abaxial collenchyma, p: pith, ph: phloem, x: xylem, cp: cortical parenchyma, sc: sclerenchyma, pm: palisade mesophyll, sm: spongy mesophyll, tr: trichomes. Scale bars: 100 µm.

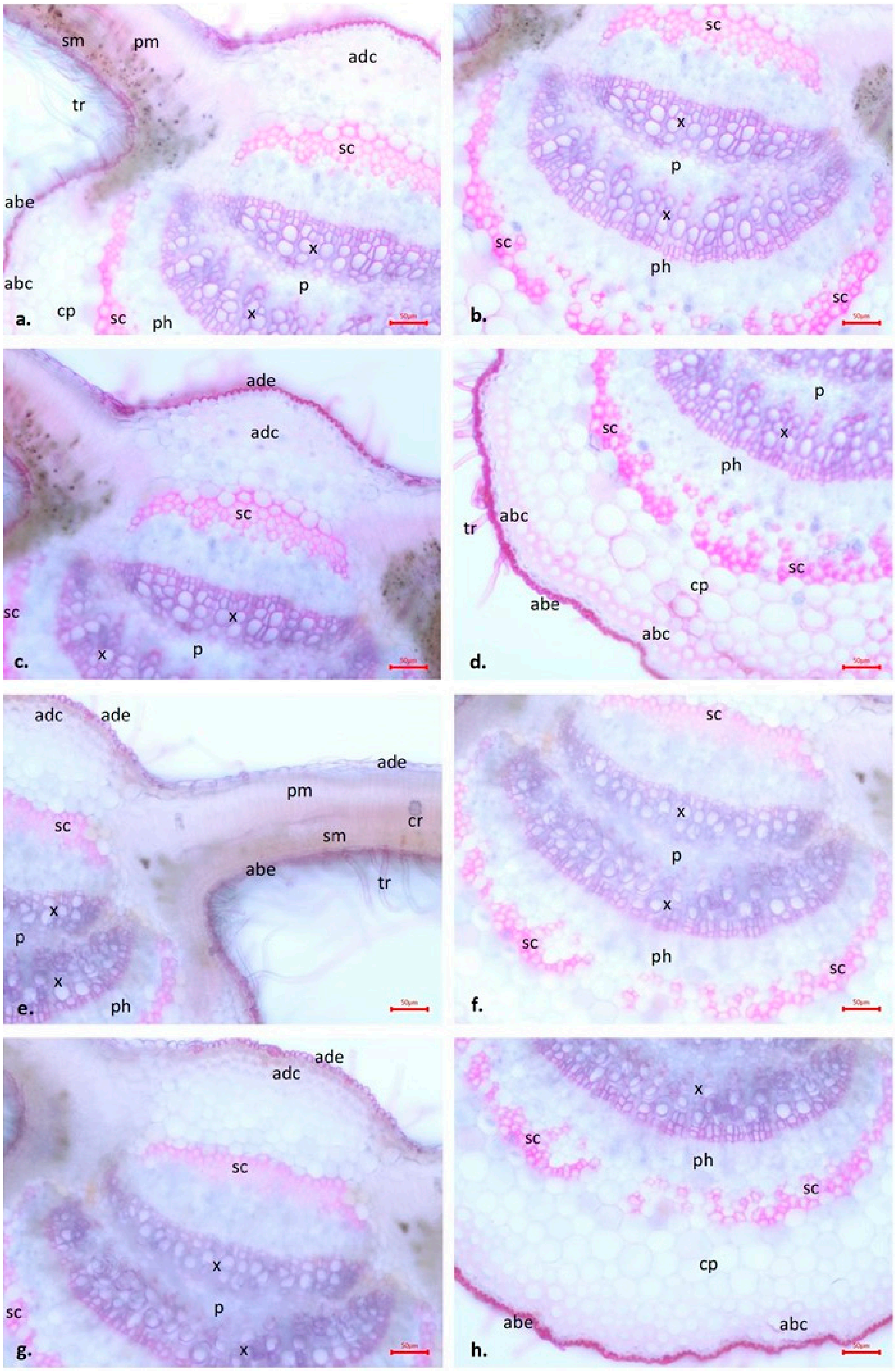

Figure 6. Effects of soil treatments on the anatomical characteristics of the midrib and vascular bundle in the case of the control and WA-treated samples. Transverse section of leaf laminas of *Salix triandra* × *S. viminalis* 'Inger'. (**a**–**d**) Control ((**a**,**b**): 10×, (**c**,**d**): 20×), (**e**–**h**) WA ((**e**,**f**): 10×, (**g**,**h**): 20×). WA = wood ash. ade: adaxial epidermis, abe: abaxial epidermis, adc: adaxial collenchyma, abc: abaxial collenchyma, sc: sclerenchyma, x: xylem, ph: phloem, p: pith, cp: cortical parenchyma, pm: palisade mesophyll, sm: spongy mesophyll, cr: Ca-oxalate crystal rosette, tr: trichomes. Scale bars: 50 µm.

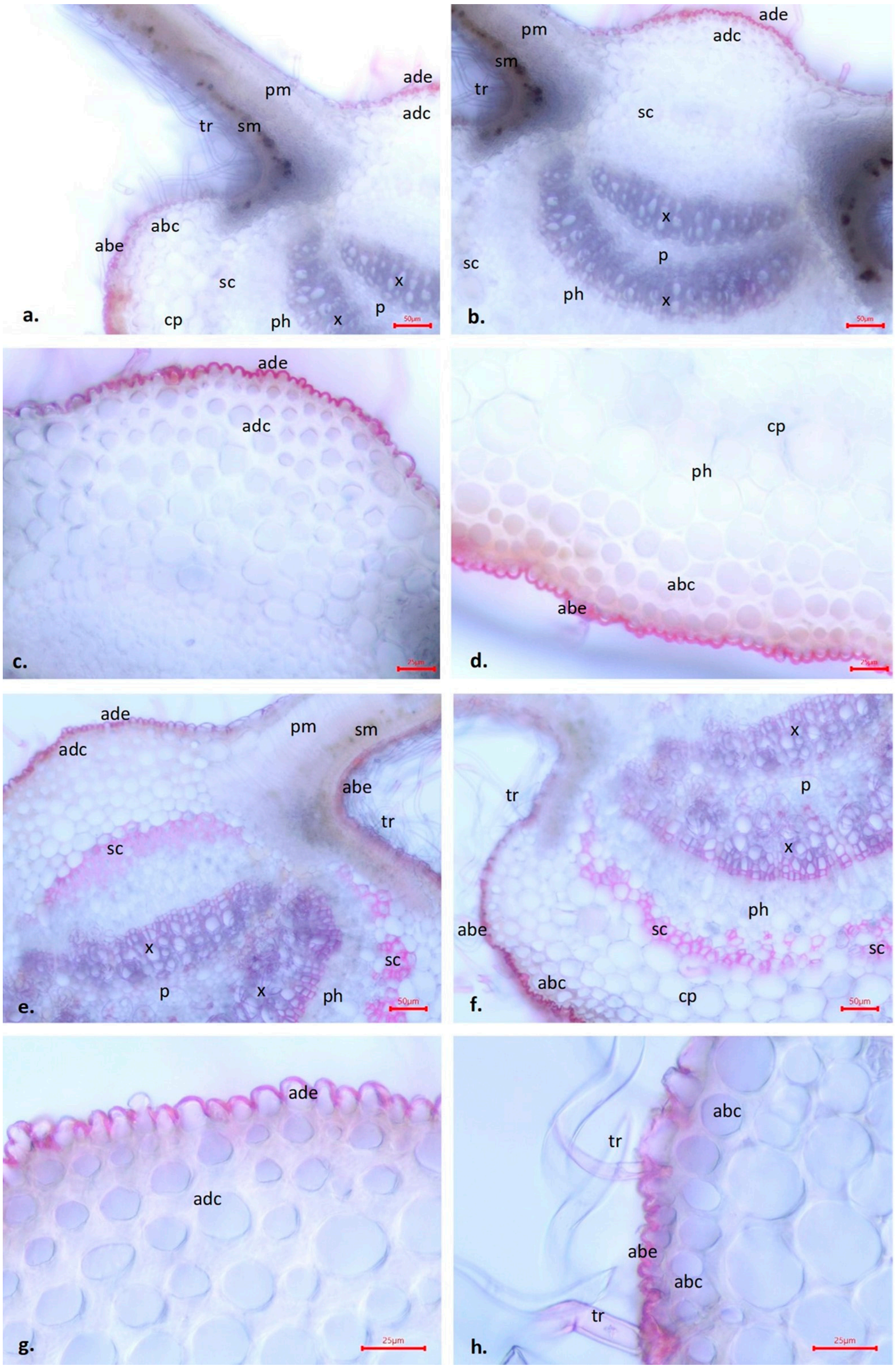

Figure 7. Effects of soil treatments on the anatomical characteristics of the midrib and vascular bundle in the case of the MSSC + MSS- and MSSC + MSS + WA-treated samples. Transverse section of leaf laminas of *Salix triandra* × *S. viminalis* 'Inger'. (**a**–**d**) MSSC + MSS ((**a**,**b**): 10×, (**c**,**d**): 20×), (**e**–**h**) MSSC + MSS + WA ((**e**,**f**): 10×, (**g**,**h**): 20×). MSSC = municipal sewage sludge compost. MSS = municipal sewage sediment. WA = wood ash. ade: adaxial epidermis, abe: abaxial epidermis, adc: adaxial collenchyma, abc: abaxial collenchyma, sc: sclerenchyma, x: xylem, ph: phloem, p: pith, cp: cortical parenchyma, pm: palisade mesophyll, sm: spongy mesophyll, tr: trichomes. Scale bars: 10×: 50 µm, 20×: 25 µm.

All treatments statistically significantly reduced the extent of both the adaxial and abaxial sclerenchymatous stock around the vascular bundle. The decrease in the extent of the sclerenchymatous stock was caused by the increase in As and Cr concentrations within the leaf. The changes in these two PTE concentrations negatively affected the extent of the sclerenchyma (As: $r = -0.9005$; Cr: $r = -0.9482$). The differences were statistically proven (Table 4). The most significant reduction was in the case of the MSSC + MSS treatment, where the extent of the adaxial sclerenchyma was reduced by 59% compared to the control. This value was almost 90% in the case of the abaxial sclerenchyma. With the WA treatment, the volume of the reduction was more moderate at 32% and 49%. In the case of the MSSC + MSS + WA treatment, the positive effects of the WA were also observable. However, the extent of the adaxial sclerenchymatous stock was significantly smaller compared to the control, although one of the abaxial stocks was significantly higher. Compared to the MSSC + MSS treatment, in the case of the MSSC + MSS + WA treatment, the area of the adaxial sclerenchymatous stock inside the leaf lamina increased by 67%, and the area of the abaxial sclerenchymatous stock increased by 13 times. A similar tendency was observed in the case of the collenchymatous stock, both in the case of adaxial and abaxial stock. Due to the MSSC + MSS + WA treatment, a significantly larger extent of collenchymatous stock was measured compared to the control and other treatments. This parameter also showed the lowest value with the MSSC + MSS treatment, and the effect of the WA treatment was only slightly negative compared to the control. However, in the case of the WA treatment, and even more prominently in the case of the MSSC + MSS + WA treatment, a significantly larger collenchyma extent compared to the MSSC + MSS treatment (in the case of the MSSC + MSS + WA treatment, the extent of adaxial collenchyma was 118%, and the abaxial one was 25% larger compared to only MSSC + MSS treatment) was measured.

Gomes et al. [63] reported an increased thickness of the abaxial and adaxial sclerenchyma. This could be related to the adsorption of metals in the cell walls of sclerenchymatous cells, as an alternative pathway for the allocation of harmful ions and preventing their translocation to photosynthetic tissues. Vollenweider [35] concluded similarly to Gomes [63] that directing the deposition of heavy metals to non-photosynthetic tissues could be a plant strategy to tolerate toxic levels of heavy metals. Vollenweider et al. [35] also observed thickened walls of the collenchymas in the *Salix* species.

During the examination of the size of the stomata, it was established that their width significantly decreased in the following order: control, MSSC + MSS, WA, and MSSC + MSS + WA (Table 4). Compared to the control, the highest increase was measured in the case of the MSSC + MSS treatment. In this case, the width of the stomata decreased by 34% on average. The WA treatment caused a significantly smaller decrease, and the usage of WA treatment as an addition to the MSSC + MSS treatment also caused a smaller reduction than the MSSC + MSS treatment.

A similar tendency was observed in the length of the stomata. In the case of this parameter, the MSSC + MSS treatment resulted in the shortest length (the length decreased by 22%). The smallest reduction was observed in the case of the WA treatment (2%). In the case of the MSSC + MSS + WA treatment, the length of the stomata decreased by 12% compared to the control.

By examining the stomatal density, it was observed that while the WA treatment reduced the size of the stomata, it also increased the number of stomata per unit. This treatment increased stomatal density the most significantly, as it increased by 96% compared to the control. Aside from the WA treatment, in all other treatments, a significantly higher stomatal density was observed compared to the control. However, the volume of the increase was significantly lower than that experienced in the case of WA treatment.

The results of Guidi Nissim et al. [64] and Labrecque and Teodorescu [65] confirm the observation from this study. They stated that the willow cultivars have impressive morphological plasticity to control water loss, and this is the likely reason why they are well-adapted to abiotic/biotic-stressed conditions (drought stress, PTE stress, UV stress, and ozone stress). Di Baccio et al. [37] showed that Zn treatments induced variations in stomatal density and size in the case of *Populus* × *euramericana*. Wuytach et al. [66], similar to our results, concluded that the white willow (*Salix alba* L.), grown in more polluted environments, adapts by forming more numerous but smaller stomata. They also established that the stomatal characteristics of white willow are potentially good bioindicators for monitoring air quality and potential toxic elements in the environment. Similar to the observation of Pataky [67], extensive changes were observed in the length/width ratio (L/W) of guard cells and the stomata number/index. Therefore, the L/W ratio of guard cells, the stomata index, and the number of stomata can be used for diagnostic aims. Similar to the above results, when using the epidermis for diagnostic aims (for example, monitoring the effects of PTEs on the properties of the leaf epidermis), the lower epidermis of the leaf affords more reliable results. Other researchers [68,69] also reported increased stomata density in leaves exposed to stress caused by PTEs. Guo et al. [29] and Melo et al. [70] found that an increase in stomata density was accompanied by a decrease in stomata size.

The results of the conducted correlation analysis showed that from the PTEs accumulated in leaves, As, Cr, Cu, and Pb have a strong negative effect on the evolution of the size of the stomata (L/W) (As: $r = -0.9576/r = -0.9409$; Cr: $r = -0.9398/r = -0.9533$; Cu: $r = -0.8569/r = -0.9074$; Pb: $r = -0.9677/r = -0.9034$). From the results of regression analysis, the effect of Ni on stomata length must be highlighted: in the examined Ni concentration range, a 0.1 mg/kg change in concentration could cause a decrease of 1.145 µm in the length of the stomata (Figure 3e). A change of 0.1 mg/kg in Cr concentration decreases stomata width by 2.079 µm (Figure 3f).

However, a strong positive correlation can be observed between the growth of the concentration of the elements within the leaves and the alteration of stomata density: As: $r = 0.9555$; Cr: $r = 0.9064$; Ni: $r = 0.9091$; Pb: $r = 0.9415$. The regression analysis confirmed the results of the correlation analysis. Arsenic and Pb must be highlighted due to their positive effect on stomata density. In the examined As concentration range, a change of 0.1 mg/kg increases stomata density by 118.16 no./mm^2, while a 0.1 mg/kg change in Pb increases stomata density by 61.822 no./mm^2 (Figure 3g,h).

4. Conclusions

The results confirmed that energy willow has good PTE phytoextraction potential. The elevated PTE content of the soil caused rapid changes in the microanatomical properties of the leaves of the examined *Salix* hybrid. Some typical changes were observed in the histological structure of leaves, such as signs of senescence. These changes indicated the PTE toxicity of the biosolid (MSSC + MSS) treatments. Protecting the energy willow from the toxic effects of PTEs in phytoremediation, the application of special soil amendments is also needed and keeps the trees in good condition. In this experiment, wood ash was able to moderate the negative effects of PTEs from wastewater solids on the microanatomical properties of leaves. As a result of WA application, the negative effect of PTE load on the leaf mesophyll and cuticle layer was minimalized, while the extent of sclerenchymatous and collenchymatous tissue within the leaf increased. It can therefore be assumed that the organic matter production of the plants used for phytoremediation of PTE-contaminated soils will not be disturbed, and the water balance of the plants will not become unstable, if biosolids are co-applied with wood ash. The increased sclerenchymatous and collenchymatous areas have high importance in the protection of the photosynthetic apparatus because the cells of these tissues can accumulate PTEs in their cell walls (forming an important line of defense). In this way, they can prevent PTEs from reaching and damaging the center of the photosynthetic apparatus. To prove this hypothesis, further research is needed. Wood ash application during the phytoremediation of the soils contaminated with PTEs can increase the active lifetime and the phytoextraction efficiency of rapidly growing energy plants (e.g., *Salix* species).

Supplementary Materials: The following supporting information can be downloaded at: https://www.mdpi.com/article/10.3390/agronomy14081625/s1. Figure S1. Scheme [2] of the long-term experiment with energy willow (*Salix triandra* × *Salix viminalis* 'Inger'), soil treatments between 2011 and 2017 in a random block layout with 4 replications (Nyíregyháza, Hungary); Figure S2. Scheme [2] of the long-term experiment with energy willow (*Salix triandra* × *Salix viminalis* 'Inger'), soil treatments during 2018 (Nyíregyháza, Hungary). Table S1. Test of normality (Kolmogorov–Smirnov Test (K–S Test)) of the microanatomical parameters of willow leaves; Table S2. Test of normality (Kolmogorov–Smirnov Test (K–S Test)) of the concentrations of potentially toxic elements (PTEs) in the leaves of energy willow (*Salix triandra* × *Salix viminalis* 'Inger'); Table S3. Correlations (r) between concentrations of potentially toxic elements in leaves of energy willow and microanatomical parameters (open-field long-term experiment with *Salix triandra* × *Salix viminalis* 'Inger'), June 2019.

Author Contributions: Conceptualization, L.S. and C.T.; methodology, L.S., C.T. and B.T.; formal analysis, L.S. and C.T.; investigation, L.S. and C.T.; data curation, L.S. and C.T.; writing—original draft preparation, C.T., L.S. and B.T.; writing—review and editing, L.S. and C.T.; visualization, L.S., C.T. and B.T.; supervision, L.S., C.T. and B.T.; resource, B.T.; project administration, L.S.; funding acquisition, L.S. All authors have read and agreed to the published version of the manuscript.

Funding: This research was funded by Hungarian R&D Competitiveness and Excellence Cooperation "Genetic utilization of plants in the Pannon region", grant number GINOP 2.2.1-15-2017-00042.

Data Availability Statement: The original contributions presented in the study are included in the article. Further inquiries can be directed to the corresponding author.

Acknowledgments: This research was supported in the frame of Hungarian GINOP 2.2.1-15-2017-00042 R&D Competitiveness and Excellence Cooperation by the "Genetic utilization of plants in the Pannon region" project. The authors appreciate the precise service of Tünde Pusztahelyi and her team in the plant and soil analysis from the Agricultural Instrument Center, University of Debrecen, Debrecen, Hungary. Support of the Scientific Council of the University of Nyíregyháza is acknowledged. The publication was supported by the University of Debrecen Program for Scientific Publication.

Conflicts of Interest: The authors declare no conflict of interest.

References

1. Smart, L.B.; Cameron, K.D. Shrub willow. In *Handbook of Bioenergy Crop Plants*; Kole, C., Joshi, C.P., Shonnard, D.R., Eds.; CRC Press: Boca Raton, FL, USA; London, UK; New York, NY, USA, 2012; pp. 687–708.
2. Simon, L.; Uri, Z.; Vigh, S.; Irinyiné Oláh, K.; Makádi, M.; Vincze, G. Phytoextraction of potentially toxic elements from wastewater solids and willow ash—Experiences with energy willow (*Salix triandra* × *S. viminalis* 'Inger'). In *Bioenergy Crops: A Sustainable Means of Phytoremediation*, 1st ed.; Puthur, J.T., Dhankher, O.P., Eds.; CRC Press/Taylor & Francis Group: Boca Raton, FL, USA, 2022; Chapter 13; pp. 227–245. ISBN 9781003043522. [CrossRef]
3. Pulford, I.D.; Riddell-Black, D.; Stewart, C. Heavy metal uptake by willow clones from sewage sludge-treated soil: The potential for phytoremediation. *Int. J. Phytoremediat.* **2002**, *4*, 59–72. [CrossRef]
4. Park, B.B.; Yanai, R.D.; Sahm, J.M.; Lee, D.K.; Abrahamson, L.P. Wood ash effects on plant and soil in a willow bioenergy plantation. *Biomass Bioenerg.* **2005**, *28*, 355–365. [CrossRef]
5. Dimitriou, I.; Eriksson, J.; Adler, A.; Aronsson, P.; Verwijst, T. Fate of heavy metals after application of sewage sludge and wood-ash mixtures to short-rotation willow coppice. *Environ. Pollut.* **2006**, *142*, 160–169. [CrossRef] [PubMed]
6. Hytönen, J. Wood ash fertilisation increases biomass production and improves nutrient concentrations in birches and willows on two cutaway peats. *Balt. For.* **2016**, *22*, 98–106.
7. Saletnik, B.; Puchalski, C. Suitability of biochar and biomass ash in basket willow (*Salix viminalis* L.) cultivation. *Agronomy* **2019**, *9*, 577. [CrossRef]
8. Gyuricza, C.; Nagy, L.; Ujj, A.; Mikó, P.; Alexa, L. The impact of composts on the heavy metal content of the soil and plants in energy willow plantations (*Salix* spp.). *Cereal Res. Commun.* **2008**, *36*, 279–282.
9. Maxted, A.P.; Black, C.R.; West, H.M.; Crout, N.M.J.; McGrath, S.P.; Young, S.D. Phytoextraction of cadmium and zinc by *Salix* from soil historically amended with sewage sludge. *Plant Soil.* **2007**, *290*, 157–172. [CrossRef]
10. Jama, A.; Nowak, W. Willow (*Salix viminalis* L.) in purifying sewage sludge treated soils. *Pol. J. Agron.* **2012**, *9*, 3–6.
11. Simon, L.; Szabó, B.; Szabó, M.; Vincze, G.; Varga, C.; Uri, Z.; Koncz, J. Effect of various soil amendments on the mineral nutrition of *Salix viminalis* and *Arundo donax* energy crops. *Eur. Chem. Bull.* **2013**, *2*, 18–21. [CrossRef]
12. Saletnik, B.; Zaguła, G.; Saletnik, A.; Bajcar, M.; Puchalski, C. Biochar and ash fertilization alter the chemical properties of basket willow (*Salix viminalis* L.). *Agronomy* **2020**, *10*, 660. [CrossRef]
13. Wójcik, M.; Stachowicz, F.; Masłoń, F. The use of wood biomass ash in sewage sludge treatment in terms of its agricultural utilization. *Waste Biomass Valori.* **2020**, *11*, 753–768. [CrossRef]

14. Vysloužilová, M.; Tlustoš, P.; Száková, P. Cadmium and zinc phytoextraction of seven clones of *Salix* spp. *planted on heavy metal contaminated soils. Plant Soil Environ.* **2003**, *49*, 542–547.
15. Berndes, F.; Fredrikson, F.; Börjesson, P. Cadmium accumulation and *Salix*-based phytoextraction on arable land in Sweden. *Agr. Ecosyst. Environ.* **2004**, *103*, 207–223. [CrossRef]
16. Dickinson, N.M.; Pulford, I.D. Cadmium phytoextraction using short-rotation coppice *Salix*: The evidence trail. *Environ. Int.* **2005**, *31*, 609–613. [CrossRef] [PubMed]
17. Simon, L.; Makádi, M.; Uri, Z.; Vigh, S.; Irinyiné Oláh, K.; Vincze, G.; Tóth, C. Phytoextraction of toxic elements and chlorophyll fluorescence in the leaves of energy willow (*Salix* spp.), treated with wastewater solids and wood ash. Agrokem Talajtan. *Agrochem. Soil Sci.* **2022**, *71*, 77–99. [CrossRef]
18. Meers, E.; Vandecasteele, B.A.; Ruttens, J. Vangronsveld and F.M.G. Tack. Potential of five willow species (*Salix* spp.) for phytoextraction of heavy metals. *Environ. Exp. Bot.* **2007**, *60*, 57–68. [CrossRef]
19. Mleczek, M.; Gąsecka, M.; Drzewiecka, K.; Goliński, P.; Magdziak, Z.; Chadzinikolau, T. Copper phytoextraction with willow (*Salix viminalis* L.) under various Ca/Mg ratios. Part 1. Copper accumulation and plant morphology changes. *Acta Physiol. Plant* **2013**, *35*, 3251–3259. [CrossRef]
20. Vandecasteele, B.; Quataert, P.; Piesschaert, F.; Lettens, S.; De Vos, B.; DuLaing, G. Translocation of Cd and Mn from bark to leaves in willows on contaminated sediments: Delayed budburst is related to high Mn concentrations. *Land* **2015**, *4*, 255–280. [CrossRef]
21. Tőzsér, D.; Harangi, S.; Baranyai, E.; Lakatos, G.; Fülöp, Z.; Tóthmérész, B.; Simon, E. Phytoextraction with *Salix viminalis* in a moderately to strongly contaminated area. *Environ. Sci. Pollut. R.* **2018**, *25*, 3275–3290. [CrossRef]
22. Tlustoš, P.; Száková, J.; Vysloužilová, M.; Pavlíková, D.; Weger, J.; Javorská, H. Variation in the uptake of arsenic, cadmium, lead, and zinc by different species of willows *Salix* spp. grown in contaminated soils. *Cent. Eur. J. Biol.* **2007**, *2*, 254–275. [CrossRef]
23. Salam, M.M.A.; Mohsin, M.; Kaipiainen, E.; Villa, A.; Kuittinen, S.; Pulkkinen, P.; Pelkonen, P.; Pappinen, A. Biomass growth variation and phytoextraction potential of four *Salix* varieties grown in contaminated soil amended with lime and wood ash. *Int. J. Phytoremediat.* **2019**, *21*, 1522–6514. [CrossRef] [PubMed]
24. Labrecque, M.; Hu, Y.; Vincent, G.; Shang, K. The use of willow microcuttings for phytoremediation in a copper, zinc and lead contaminated field trial in Shanghai, China. *Int. J. Phytoremediat.* **2020**, *22*, 1331–1337. [CrossRef] [PubMed]
25. Greger, M.; Landberg, T. Use of willow in phytoextraction. *Int. J. Phytoremediat.* **1999**, *1*, 115–123. [CrossRef]
26. Pulford, I.D.; Watson, C. Phytoremediation of heavy metal contaminated land by trees—A review. *Environ. Int.* **2003**, *29*, 529–540. [CrossRef] [PubMed]
27. Marschner, H. *Mineral Nutrition of Higher Plants*; Academic Press: Cambridge, MA, USA; Harcourt Brace and Company Publishers: London, UK, 1995.
28. Binns, W.W.; Blunden, G. Comparative anatomy of *Salix* species and hybrids. *Bot. J. Linn. Soc.* **2008**, *81*, 205–214. [CrossRef]
29. Guo, Z.; Gao, Y.; Yuan, X.; Yuan, M.; Huang, L.; Wang, S.; Liu, C.; Duan, C. Effects of Heavy Metals on Stomata in Plants: A Review. *Int. J. Mol. Sci.* **2023**, *24*, 9302. [CrossRef] [PubMed]
30. Almotairy, H. Heavy Metal Contamination in Soil: Implications for Crop Resilience and Abiotic Stress Management [Internet]. In *Abiotic Stress in Crop Plants—Ecophysiological Responses and Molecular Approaches*; IntechOpen: Rijeka, Croatia, 2024. [CrossRef]
31. El-Khatib, A.A.; El-Shanawany, A.A.; El-Amery, E.M. Tree leaf as bio-indicator for air pollution around superphosphate fertilizers plant. *Egypt J. Ecol. Health Environ.* **2016**, *4*, 95–101. [CrossRef]
32. Khalili, Z.; Maassoumi, A.A.; Ghahremaninejad, F.; Mirzaie-Nodoushan, H. Foliar anatomy of some *Salix* species (Salicaceae) in Iran. *Iran. J. Bot.* **2010**, *16*, 293–302.
33. Hermle, S.; Vollenweider, P.; Günthardt-Goerg, M.S.; McQuattie, C.J.; Matyssek, R. Leaf responsiveness of *Populus tremula* and *Salix viminalis* to soil contaminated with heavy metals and acidic rainwater. *Tree Physiol.* **2007**, *27*, 1517–1531. [CrossRef] [PubMed]
34. André, O.; Vollenweider, P.; Günthardt-Goerg, M.S. Foliage response to heavy metal contamination in Sycamore Maple (*Acer pseudoplatanus* L.). *For. Snow Landsc. Res.* **2006**, *80*, 275–288.
35. Vollenweider, P.; Cosio, C.; Günthardt-Goerg, M.S.; Keller, C. Localization and effects of cadmium in leaves of cadmium-tolerant willow (*Salix viminalis* L.) Part II Microcolonization and cellular effects of cadmium. *Environ. Exp. Bot.* **2006**, *58*, 25–40. [CrossRef]
36. Nikolić, N.; Zorić, L.; Cvetković, I.; Pajević, S.; Borišev, M.; Orlović, S.; Pilipović, A. Assessment of cadmium tolerance and phytoextraction ability in young *Populus deltoides* L. and *Populus* × *euramericana* plants through morpho-anatomical and physiological responses to growth in cadmium enriched soil. *iForest* **2017**, *10*, 635–644. [CrossRef]
37. Di Baccio, D.; Minnocci, A.; Sebastiani, L. Leaf structural modifications in *Populus* × *euramericana* subjected to Zn excess. *Biol. Plant.* **2010**, *54*, 502–508. [CrossRef]
38. Luković, J.; Merkulov, L.; Pajević, S.; Zorić, L.; Nikolić, N.; Borišev, M.; Karanović, D. Quantitative assessment of effects of cadmium on the histological structure of poplar and willow leaves. *Water Air Soil Pollut.* **2012**, *223*, 2979–2993. [CrossRef]
39. Shi, G.R.; Cai, Q.S. Photosynthetic and anatomic responses of peanut leaves to cadmium stress. *Photosynthetica* **2008**, *46*, 627–630. [CrossRef]
40. Stoláriková-Vaculíková, M.; Romeo, S.; Minnocci, A.; Luxová, M.; Vaculík, M.; Sebastiani, L. Anatomical, biochemical and morphological responses of poplar *Populus deltoides* clone Lux to Zn excess. *Environ. Exp. Bot.* **2015**, *109*, 235–243. [CrossRef]
41. Al Afas, N.; Marron, N.; Ceulemans, R. Variability in *Populus* leaf anatomy and morphology in relation to canopy position, biomass production, and varietal taxon. *Ann. For. Sci.* **2007**, *64*, 521–532. [CrossRef]

42. Bini, C.; Wahsha, M.; Fontana, S.; Maleci, L. Effects of heavy metals on morphological characteristics of *Taraxacum officinale* Web. growing on mine soils in NE Italy. *J. Geochem. Explor.* **2012**, *123*, 101–108. [CrossRef]
43. da Silva de Jesus, D.; Martins, F.M.; de Azevedo Neto, A.D. Structural changes in leaves and roots are anatomical markers of aluminum sensitivity in sunflower. *Pesq. Agropec. Trop. Goiânia* **2016**, *46*, 383–390. [CrossRef]
44. Simon, L.; Makádi, M.; Vincze, G.; Uri, Z.; Irinyiné Oláh, K.; Zsombik, L.; Vígh, S.; Szabó, B. Long-term field fertilization experiment with energy willow (*Salix* spp.)—Elemental composition and chlorophyll fluorescence in the leaves. *Agrokem Talajt.* **2018**, *67*, 91–103. [CrossRef]
45. *MSZ 21470-50*; Environmental Testing of Soils. Determination of Total and Soluble Toxic Element, Heavy Metal and Chromium(VI) Content. Hungarian Standards Board: Budapest, Hungary, 2006. (In Hungarian)
46. Hungarian Kvvm-Eüm-Fvm Joint Decree No. 6/2009. (IV. 14.) of the Ministry of Environment and Water Management, Ministry of Health, Ministry of Agriculture on the Threshold Limits and Measurement of Pollutants Necessary to Protect the Geological Medium and Groundwater against Pollution. Available online: https://net.jogtar.hu/jogszabaly?docid=a0900006.kvv (accessed on 23 July 2024). (In Hungarian).
47. Barykina, R.P. *Guide on Botanical Microtechique*; Base and Methods; MSU: Moscow, Russia, 2004; p. 312.
48. Tóth, C.; Simon, L.; Tóth, B. Microanatomical changes in the leaves of *Arundo donax* (L.) caused by potentially toxic elements from municipal sewage sediment. *Plants* **2024**, *13*, 740. [CrossRef] [PubMed]
49. Hilu, K.W.; Randall, J.L. Convenient method for studying grass leaf epidermis. *Taxon* **1984**, *33*, 413–415. [CrossRef]
50. Gardner, S.D.L.; Taylor, G.; Bosac, C. Leaf growth of hybrid poplar following exposure to elevated CO_2. *New Phytol.* **1995**, *131*, 81–90. [CrossRef] [PubMed]
51. Elagöz, V.; Han, S.S.; Manning, W.J. Acquired changes in stomatal characteristics in response to ozone during plant growth and leaf development of bush beans (*Phaseolus vulgaris* L.) indicate phenotypic plasticity. *Environ. Poll.* **2006**, *140*, 395–405. [CrossRef] [PubMed]
52. Ceulemans, R.; Impens, I.; Steenackers, V. Variations in photosynthetic, anatomical, and enzymatic leaf traits and correlations with growth in recently selected *Populus* hybrids. *Can. J. For. Res.* **1987**, *17*, 273–283. [CrossRef]
53. Tóth, C.; Irinyiné-Oláh, K.; Simon, L. The effect of sewage sediment containing toxic elements on the microanatomy of the leaf of *Sorghum* species. In *International Multidisciplinary Conference*, 14th ed.; Páy, G.L., Ed.; University of Nyíregyháza: Nyíregyháza, Hungary, 2022; pp. 124–133.
54. Tóth, C.; Vincze, G.; Irinyiné-Oláh, K.; Uri, Z.; Vigh, S.; Simon, L. The effect of toxic elements on the microanatomy of the leaves of the *Salix alba* L. *Rev. Agricult. Rural Develop.* **2022**, *11*, 139–145. [CrossRef]
55. García-Gutiérrez, E.; Ortega-Escalona, F.; Angeles, G. A novel, rapid technique for clearing leaf tissues. *Appl. Plant Sci.* **2020**, *8*, e11391. [CrossRef] [PubMed]
56. Sass, J.E. *Botanical Microtechnique*, 2nd ed.; Iowa State College Press: Ames, IA, USA, 1951.
57. Kabata-Peendias, A. *Trace Elements in Soils and Plants*, 4th ed.; CRC Press: Boca Raton, FL, USA; Taylor & Francis Group: Boca Raton, FL, USA, 2011.
58. Simon, L. Potentially harmful elements in agricultural soils. In *PHEs, Environment and Human Health. Potentially Harmful Elements in the Environment and the Impact on Human Health*; Bini, C., Bech, J., Eds.; Springer: Dordrecht, The Netherlands; Heidelberg, Germany; New York, NY, USA; London, UK, 2014; pp. 85–137, 142–150.
59. Cooper, R.L.; Cass, D.D. A comparative epidermis study of the Athabasca sand dune willows (*Salix*; Salicaceae) and their putative progenitors. *Can. J. Bot.* **2003**, *81*, 749–754. [CrossRef]
60. Ghahremaninejad, F.; Khalili, Z.; Maassoumi, A.A.; Mirzaie-Nodoushan, H.; Riahi, M. Leaf epidermal features of *Salix* species (Salicaceae) and their systematic significance. *Am. J. Bot.* **2012**, *99*, 769–777. [CrossRef]
61. Fontana, M.; Labrecque, M.; Collin, A.; Bélanger, N. Stomatal distribution patterns change according to leaf development and leaf water status in *Salix miyabeana*. *Plant Growth Regul.* **2017**, *81*. [CrossRef]
62. Krzesłowska, M.; Mleczek, M.; Luboński, A.; Weręża, K.; Woźny, A.; Goliński, P.; Samardakiewicz, S. Alterations in the anatomy and ultrastructure of leaf blade in norway maple (*Acer platanoides* L.) growing on mining sludge: Prospects of using this tree species for phytoremediation. *Plants* **2024**, *13*, 1295. [CrossRef] [PubMed]
63. Gomes, P.; de Sá e Melo Marques, T.C.L.L.; de Oliveira Gonçalves Nogueira, M.; de Castro, E.M.; Soares, A.M. Ecophysiological and anatomical changes due to uptake and accumulation of heavy metal in *Brachiaria decumbens*. *Marcelo Sci. Agric.* **2011**, *68*, 566–573. [CrossRef]
64. Guidi Nissim, W.; Pitre, F.E.; Teodorescu, T.I.; Labrecque, M. Long-term biomass productivity of willow bioenergy plantations maintained in southern Quebec, Canada. *Biomass Bioenerg.* **2013**, *56*, 361–369. [CrossRef]
65. Labrecque, M.; Teodorescu, I.T. Field performance and biomass production of 12 willow and poplar clones in short-rotation coppice in southern Quebec (Canada). *Biomass Bioenerg.* **2005**, *29*, 1–9. [CrossRef]
66. Wuytack, T.; Verheyen, K.; Wuyts, K.; Kardel, F.; Adriaenssens, S.; Samson, R. The potential of biomonitoring of air quality using leaf characteristics of white willow (*Salix alba* L.). *Environ. Monit Assess* **2010**, *171*, 197–204. [CrossRef] [PubMed]
67. Pataky, S. Comparison of the leaf epidermis of *Salix alba* L. *in different regions of the leafy crown. Acta Biol. Szeged* **1969**, *15*, 29–36.
68. Baryla, A.; Carrier, P.; Franck, F.; Coulomb, C.; Sahut, C.; Havaux, M. Leaf cloroses in oilseed rape plants (*Brassica napus*) grown o cadmiumpolluted soil: Causes and consequences for photosynthesis and growth. *Planta* **2001**, *212*, 696–709. [CrossRef] [PubMed]

69. Chardonnens, A.N.; Ten Bookum, W.M.; Kuijper, D.J.; Verkleij, J.A.C.; Ernst, W.H.O. Distribution of cadmium in leaves of cadmium tolerant and sensitive ecotypes of *Silene vulgaris*. *Physiol. Plant.* **1998**, *104*, 75–80. [CrossRef]
70. Melo, H.C.; Castro, E.M.; Soares, A.M.; Melo, L.A.; Alves, J.D. Anatomical and physiological alterations in *Setaria anceps* Stapf ex Massey and *Paspalum paniculatum* L. under water deficit conditions. *Hoehnea* **2007**, *34*, 145–153, (In Portuguese, with Abstract in English). [CrossRef]